In presenting the dissertation as a partial fulfillment of the requirements for an advanced degree from the Georgia Institute of Technology, I agree that the Library of the Institution shall make it available for inspection and circulation in accordance with its regulations governing materials of this type. I agree that permission to copy from, or to publish from, this dissertation may be granted by the professor under whose direction it was written, or, in his absence, by the Dean of the Graduate Division when such copying or publication is solely for scholarly purposes and does not involve potential financial gain. It is understood that any copying from, or publication of, this dissertation which involves potential financial gain will not be allowed without written permission.

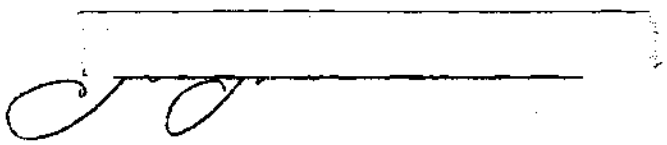

THE INFLUENCE OF RESONANT ACOUSTIC VIBRATIONS ON THROUGH-FLOW DRYING OF TUFTED TEXTILE MATERIALS

A THESIS

Presented to

The Faculty of the Graduate Division

by

Jerry Russell Dunn

In Partial Fulfillment

of the Requirements for the Degree

Master of Science in Mechanical Engineering

Georgia Institute of Technology

September, 1964

THE INFLUENCE OF RESONANT ACOUSTIC VIBRATIONS ON THROUGH-FLOW DRYING OF TUFTED TEXTILE MATERIALS

Approved: _____

_____

Chairman _____

_____

Date approved by Chairman: 11-9-64

ACKNOWLEDGMENTS

The author wishes to express his appreciation to his advisor, Dr. Kenneth R. Purdy, for the advice, support, and encouragement which he has rendered and to Dr. Charles W. Gorton and Dr. Henderson C. Ward for their service on the reading committee.

Special gratitude is expressed to Mr. Don Brock for his invaluable assistance in the design of the test equipment and in obtaining the experimental data.

The assistance of Mr. Joseph Doyal and Mr. Lewis Cavalli in assembling the test equipment was also greatly appreciated. The author is grateful to the School of Mechanical Engineering for the use of its equipment during the investigation.

Finally, the author would like to express his deepest gratitude to his wife for her patience and understanding and to his parents for their contributions to his success.

TABLE OF CONTENTS

(Continued)

TABLE OF CONTENTS (Concluded)

LIST OF TABLES

LIST OF ILLUSTRATIONS

(Continued)

LIST OF ILLUSTRATIONS (Concluded)

NOMENCLATURE

Symbol

A - area of duct, $ft.^2$

C - speed of sound in air, ft./sec.

f - frequency of oscillation of sound wave, cycles/sec. (cps)

I - per cent increase in drying rate

p - partial pressure of water vapor, psia

P - sound pressure exerted by pressure pulse

$\bar{P}$ - root-mean-square sound pressure

Q - volumetric flow rate, cfm

SPL - sound-pressure level, decibels (db)

t - temperature, °F

T - period of sound wave oscillation, sec.

U - particle velocity due to sound wave, ft./sec.

V - average through-flow velocity, ft./sec.

X - moisture content of material, lb. moisture/lb. room dry sample

Greek Letters

λ - wavelength of sound wave, ft.

ω - circular frequency = $2\pi f$, radians/sec.

Subscripts

c - refers to critical moisture content

d - refers to dry-bulb temperature

e - refers to equilibrium moisture content

(Continued)

NOMENCLATURE (Concluded)

Subscripts

o - refers to maximum amplitude of property

w - refers to wet-bulb temperature

SUMMARY

The purpose of this investigation was to determine the effect of a resonant acoustic field on the through-flow drying of tufted textile materials. This investigation, which included the effects of a resonant sound field, was an extension of the study made by Brock (3) on through-flow drying.

Two tufted carpet samples were dried at flow rates ranging from 300 to 800 cfm under the influence of a resonant sound field whose intensity was varied from no sound to a maximum value of 141 db. Drying rate curves for resonant sound conditions were compared with one for a no sound condition at the same free stream temperature, flow rate, and initial moisture content of the sample.

This comparison of drying rate curves showed the drying rate during the constant rate period increased with increasing sound-pressure level. Increases in drying rate of up to 22 per cent were obtained. Graphical representation of the data showed the increase in drying rates during the constant rate period to increase linearly with the ratio of a sound Reynolds number, Re_s, based on the maximum amplitude of the sound particle velocity to a through-flow Reynolds number, Re_{tf}, based on the average through-flow velocity. No increases in drying rates above 5 per cent were obtained for values of Re_s/Re_{tf} less than 0.23.

A plot of local sound-pressure level versus time along with moisture content of the sample versus time during a drying run showed rapid increases in sound-pressure level until the critical moisture

content was reached. After this the rate of increase began to decrease and reached a peak as the sample became dry. This indicated that the absorption by the sample of a portion of the acoustic energy radiated contributed to the increase in drying rates. However, a comparison of the energy input to the horn and the amount required to produce the increase in drying rates showed absorption was not the dominant factor contributing to the increase in drying rates.

The critical moisture content was observed to increase with increasing drying rates.

CHAPTER I

INTRODUCTION AND HISTORICAL BACKGROUND

The possibility of the use of acoustic sound fields for industrial drying applications has been recognized since P. Greguss (5) applied acoustics to a drying problem involving raw cotton. With this beginning, other applications have been found such as the processing of heat sensitive chemicals, drying of fresh wood, and the processing of photographic films.

The efficiency of energy conversion and cost of powerful sound generators has caused many possible commercial applications to develop slowly. Hueter and Bolt (8) state that a maximum electroacoustic conversion of 30 to 50 per cent can be expected for electroacoustic transducers and Boucher (2) reports that the efficiency of rotary sirens can range from 20 to 50 per cent, but in practice it is usually closer to the first figure. However, recent advances in the design of high-intensity sound generation equipment have made the application of acoustic drying techniques to practical situations more economical.

Statement of Intent

The investigation of the through-flow drying of tufted textile materials was begun in the Georgia Institute of Technology Mechanical Engineering Laboratories in 1962 by Brock (3).

It is the purpose of this investigation to extend this study to a determination of the effect of a resonant acoustic sound field on the

through-flow drying of tufted textile materials. Emphasis will be placed on the effect of sound intensity on the various regions of the drying curve, the critical moisture content, and overall drying time. These results will be compared with similar drying runs without the acoustic field.

Mechanism of Drying

The term drying refers to the removal of moisture from a substance. However, mechanical removal such as by extractors is generally not considered to be drying (12). In this restricted sense, drying will take place under the action of two mechanisms, heat transfer and diffusion. The material to be considered will be a porous material capable of absorbing moisture and through which air may be passed. Since this investigation is concerned with the drying of a substance under the influence of a moving air stream, a net air flow through the porous material will be assumed to exist in the discussion of the drying mechanism. Also, the moisture to be removed will be assumed to be water.

Drying by Heat Transfer

Drying by heat transfer may be accomplished by transferring sufficient energy to vaporize the moisture in the substance. This could be achieved in the following ways: by heat conduction from an air stream at a temperature greater than that of the sample, or by the absorption of energy within the sample. The energy could also be generated from an exterior source such as radiant or microwave heaters or possibly from an acoustic sound generator. The latter mechanism will be discussed in greater detail when a resonant sound field is explained.

Drying by Diffusion

Diffusion is the transport of a specie through a medium relative to other species in the medium. The most significant driving force for this transport is a gradient in the molal concentration profile of the specie in the medium. Just as heat transfer takes place so as to reduce temperature gradients, diffusion takes place so as to reduce molal concentration gradients. As a consequence of Dalton's law of partial pressures, it can be shown that the mole fraction and partial pressure ratio for a specie are equal for a mixture of ideal gases. Therefore, if a wet porous substance was exposed to an air stream at sufficiently low relative humidity, a diffusion of water vapor would take place between the material and the air stream until equilibrium was reached between the partial pressure of the water vapor in the material and the partial pressure of the water vapor in the free stream.

The mechanism of drying can best be explained by looking at a typical equilibrium moisture curve for a substance as shown in Figure 1. This curve plots relative humidity of the gas versus the moisture content of the substance. The moisture in a porous material will have some equilibrium partial pressure. If the material is then exposed to an air stream whose water vapor is at a partial pressure p corresponding to the relative humidity A as shown in Figure 1, the material will lose or gain moisture until the water vapor within the material has a partial pressure p in equilibrium with that of the approaching air stream. The material would have then reached its equilibrium moisture content X_e corresponding to point D in Figure 1. No further lowering of the moisture content of the substance could be obtained by exposing the

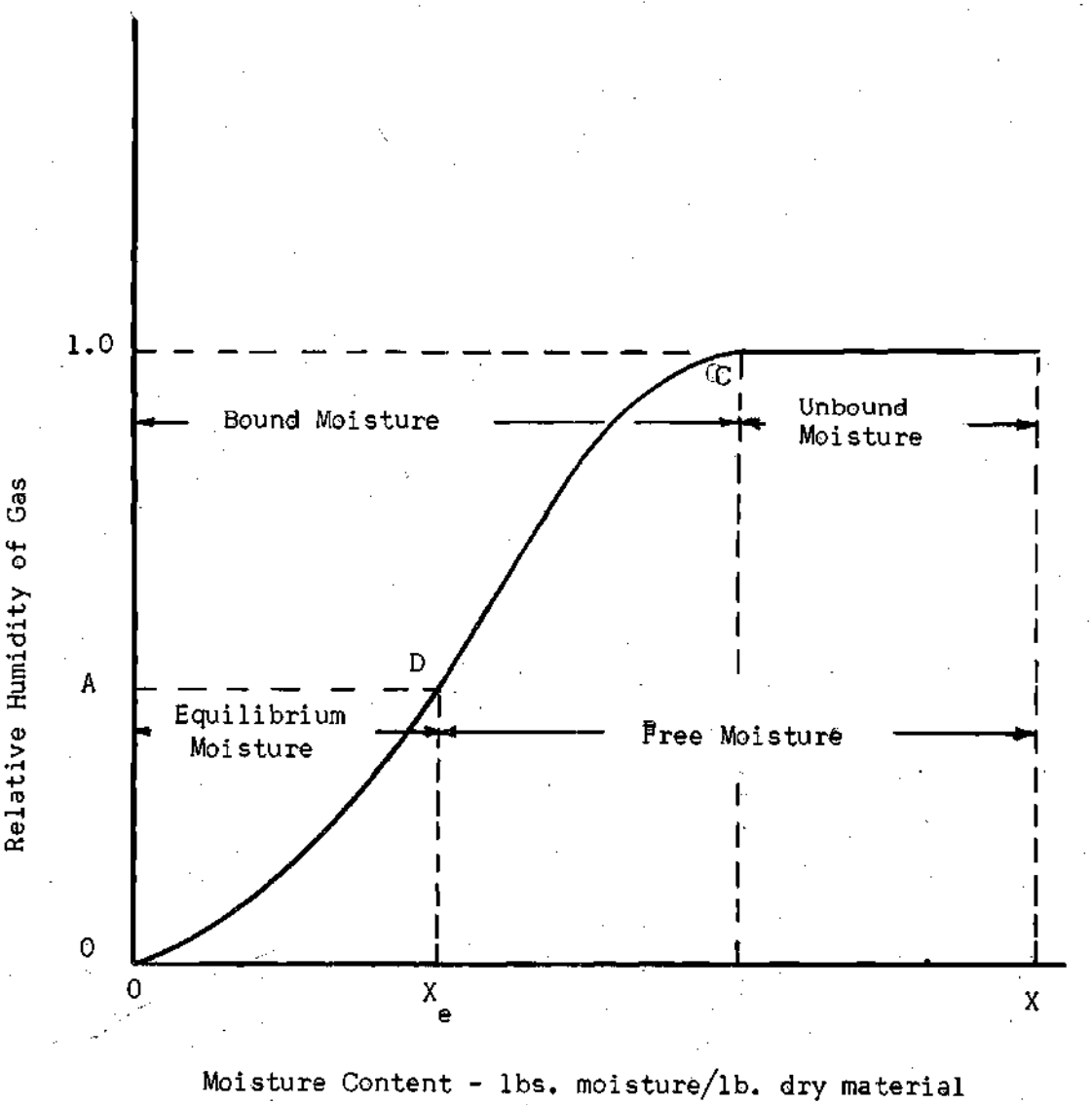

Figure 1. Equilibrium Moisture Curve.

material to the same air stream. Thus the dryness of a particular product is relative to the environment into which the moisture is being transferred.

For convenience, certain terms and definitions used to describe moisture content of substances are summarized below as given by Treybal (12).

> Moisture content, dry basis - The pounds of moisture in the substance per pound of dry solid.
>
> Equilibrium moisture - The moisture content of a substance when at equilibrium with a given partial pressure of the vapor.
>
> Bound moisture - The moisture contained by a substance which exerts an equilibrium vapor pressure less than that of the pure liquid at the same temperature.
>
> Unbound moisture - The moisture contained by a substance which exerts an equilibrium vapor pressure equal to that of the pure liquid at the same temperature.
>
> Free moisture - That moisture contained by a substance in excess of the equilibrium moisture.

The portions of the equilibrium moisture curve which pertain to the above definitions are shown in Figure 1. Therefore from Figure 1, it is seen that only the free moisture can be evaporated from a material which is exposed to a gas of relative humidity A.

A second curve useful in understanding the drying mechanism is a rate of drying curve. A typical rate of drying curve is shown in Figure 2. The initial adjustment period shown in Figure 2 is a period in which the temperature of the moisture in the substance adjusts to the saturation temperature corresponding to the partial pressure exerted by the water vapor in the material. This temperature remains constant throughout the unbound region of drying. Thus, the moisture on the

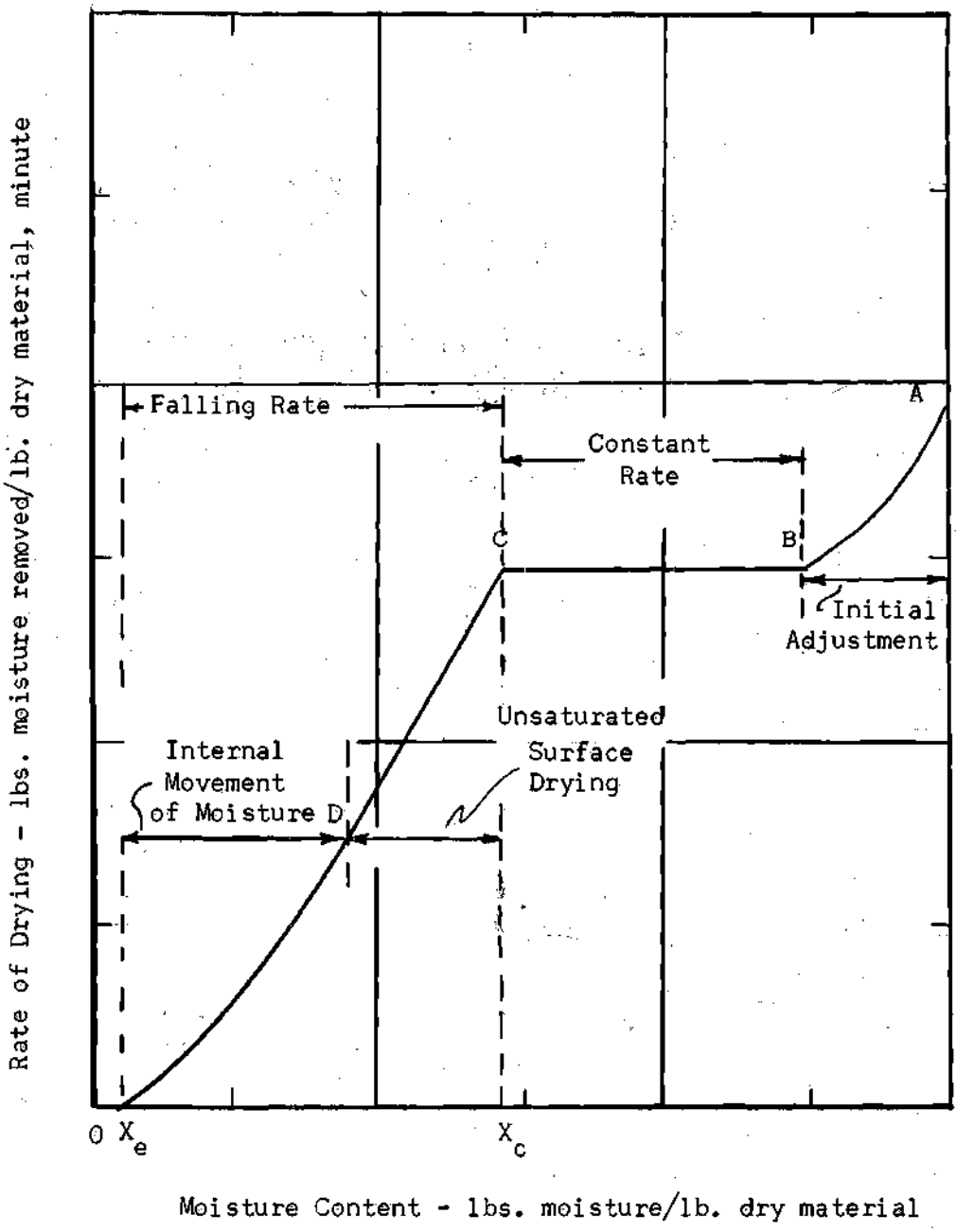

Figure 2. Typical Rate of Drying Curve.

surface of the material is in the form of a saturated liquid at a constant partial pressure during the unbound region.

The constant rate period between points B and C can be explained by observing that the driving potential for the heat-transfer mechanism, the temperature difference between the free stream and the sample, remains constant during the constant rate period as does the driving potential for the diffusion process, the difference in the mole fraction of the water vapor in the material and the water vapor in the free stream since the mole fraction is related to the partial pressure as stated previously. The substance drys at a constant rate until it reaches its critical moisture content X_c shown on Figure 2.

When some portion of the surface becomes free of saturated moisture, the material enters the falling rate period at the critical moisture content. The instantaneous rate of drying then decreases as shown to the point D where the surface has then become dry. The remaining portion of the drying curve depends upon the rate of internal diffusion of moisture to the surface and then into the free stream. The material is considered dry when the remaining internal moisture reaches pressure equilibrium with the water vapor in the approaching free stream. The substance has then reached its equilibrium moisture content as given by point D of Figure 1.

Resonant Acoustic Sound Field

The concept and terminology used in describing a resonant acoustic sound field will be presented by investigating the characteristics of a resonant sound field in a tube of finite length. When a small pressure disturbance is created in air, it is propagated throughout the medium at

the speed of sound. As the pressure pulse passes some point in space, it imparts an instantaneous velocity U and pressure P to the particles of air. If this pressure pulse is generated by a harmonic oscillator, the particles will exhibit harmonic motion and the sound wave produced by this motion will be in the form of a sine wave. The form of this wave is shown in Figure 3 where P is now the instantaneous amplitude of the deviation of the pressure pulse from the mean static pressure.

The form of the velocity wave is exactly the same as that in Figure 3 except the velocity wave is 90° out of phase with the pressure wave. Parameters which will be used to describe sound waves are:

f - frequency in cycles per second
ω - circular frequency = $2\pi f$
λ - wave length in feet
T - period of oscillation in seconds.

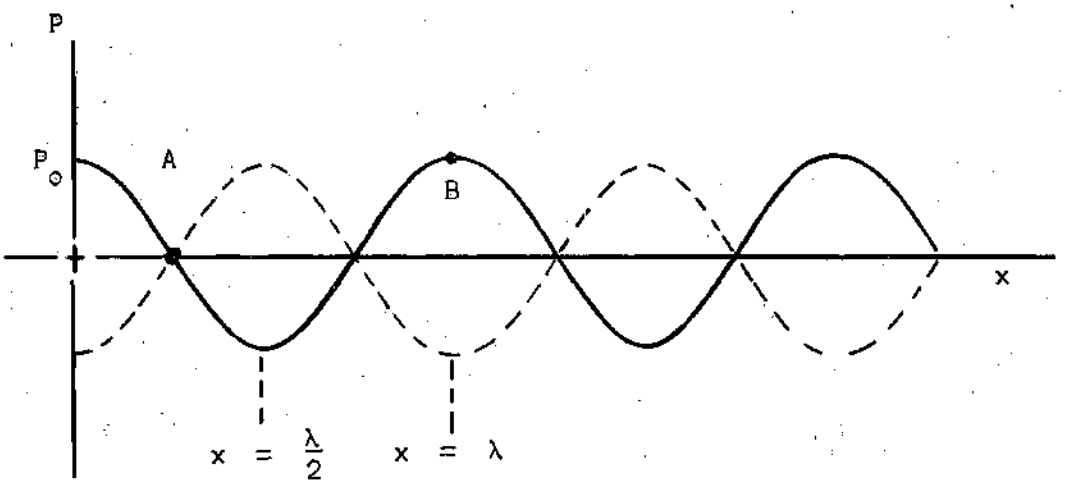

Figure 3. Pressure Variation of Imposed Sound Field.

The standard unit of measure for the sound-pressure level of a sound wave is the decibel (db). This unit relates the root-mean-square sound pressure to a reference sound pressure by the relation

$$\text{Sound-pressure level (SPL)} = 20 \log \frac{\bar{p}}{p_{ref}} \qquad (1.1)$$

where p_{ref} is the reference sound-pressure level (0.0002 microbar), and $\bar{p}$, the sound pressure, is the root-mean-square of the deviation of the total pressure from the mean static pressure.

If a sinusoidal sound wave is generated in a tube, the wave will propagate down the tube under the conditions mentioned above. If the tube is finite in length, the generated wave will be reflected and the two wave forms will then add vectorially. The sound-pressure level will either decrease or increase if the frequency of the generated wave is varied. By varying the frequency so as to cause the sound-pressure level to increase while holding the power supply constant, a condition of maximum sound pressure will be reached. At this point, the forward traveling wave and reflected wave will be in phase. The tube is now said to be in resonance. A point in the tube having no imposed pressure due to the sound field will continue to have no fluctuating pressure components. This is shown graphically in Figure 3 by point A and is called a pressure node. Point B having a maximum amplitude p_o of pressure fluctuation is called a pressure antinode. Analogous definitions are given to velocity nodes and antinodes shown in Figure 4 by points C and D respectively. When the tube is in resonance, the position of the nodes and antinodes remain fixed in the tube and the frequency for which resonance

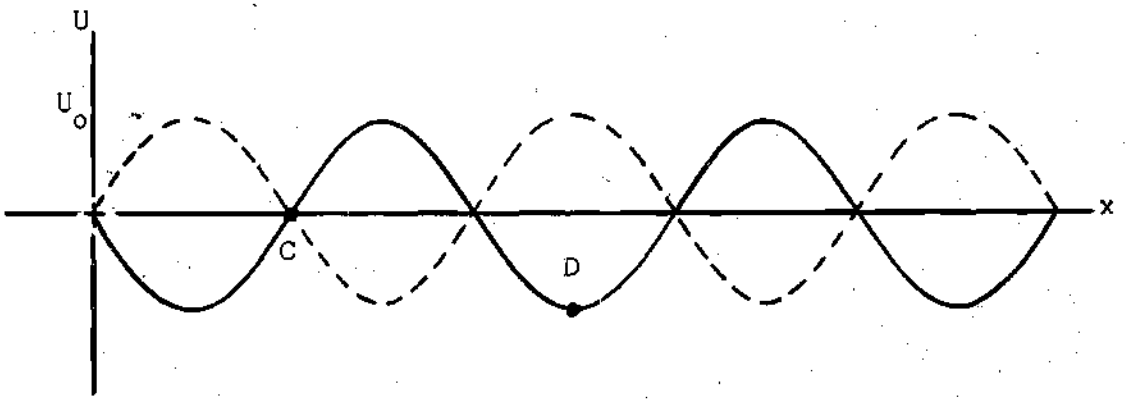

Figure 4. Velocity Variation of Imposed Sound Field.

exists is a natural frequency of the tube. The amplitude of the particle velocity, U_o, due to a sound wave in air (10) is calculated by the relation

$$\frac{U_o}{C} = 0.2 \times 10^{\{(SPL - 180)/20\}} \frac{29.92}{P_{static}} \qquad (1.2)$$

where C is the local speed of sound in air and SPL the local sound-pressure level at a pressure antinode.

It is now seen that by placing a porous material in a resonating tube at a point corresponding to point B of Figure 3, the material could be dried under the condition of a fluctuating pressure field while if the sample was placed in a position corresponding to point D of Figure 4, it could be dried under the condition of a fluctuating velocity field.

Formulation of Model

The material to be dried will be a tufted carpet as shown in Figure 5 (photograph of sample number three). Tufted carpet normally consists of a jute backing into which tufts of cotton, nylon, or wool yarn are placed.

The net air flow was made to pass through the carpet so that the tufts were positioned parallel to the direction of air flow.

The model to be studied was taken as porous cylinders of moistened yarn with axes parallel to the direction of the air stream as shown in Figure 6.

Survey of Related Literature

The first factor affecting the drying of carpet is that of heat-transfer rate. The study of effects of vibration and pulsating flows on transport phenomena was begun with the study of the effect of mechanical vibration upon the rate of heat transfer from horizontal tubes. The tubes were mechanically vibrated in the vertical direction while in a constant temperature water bath. Martinelli and Boelter (9) reported in 1938 that the heat-transfer coefficient was unaffected by mechanical vibrations of low intensity due to the dominance of free convection, but for sufficiently intense vibrations, the heat-transfer coefficient was observed to increase by as much as 400 per cent of its value without vibrations.

Fand and Kaye (7) studied the influence of an induced sound field on free convection from horizontal tubes where the sound field was normal to the tube axis and found that the heat-transfer coefficient was increased by as much as a factor of three to that in the absence of sound. There

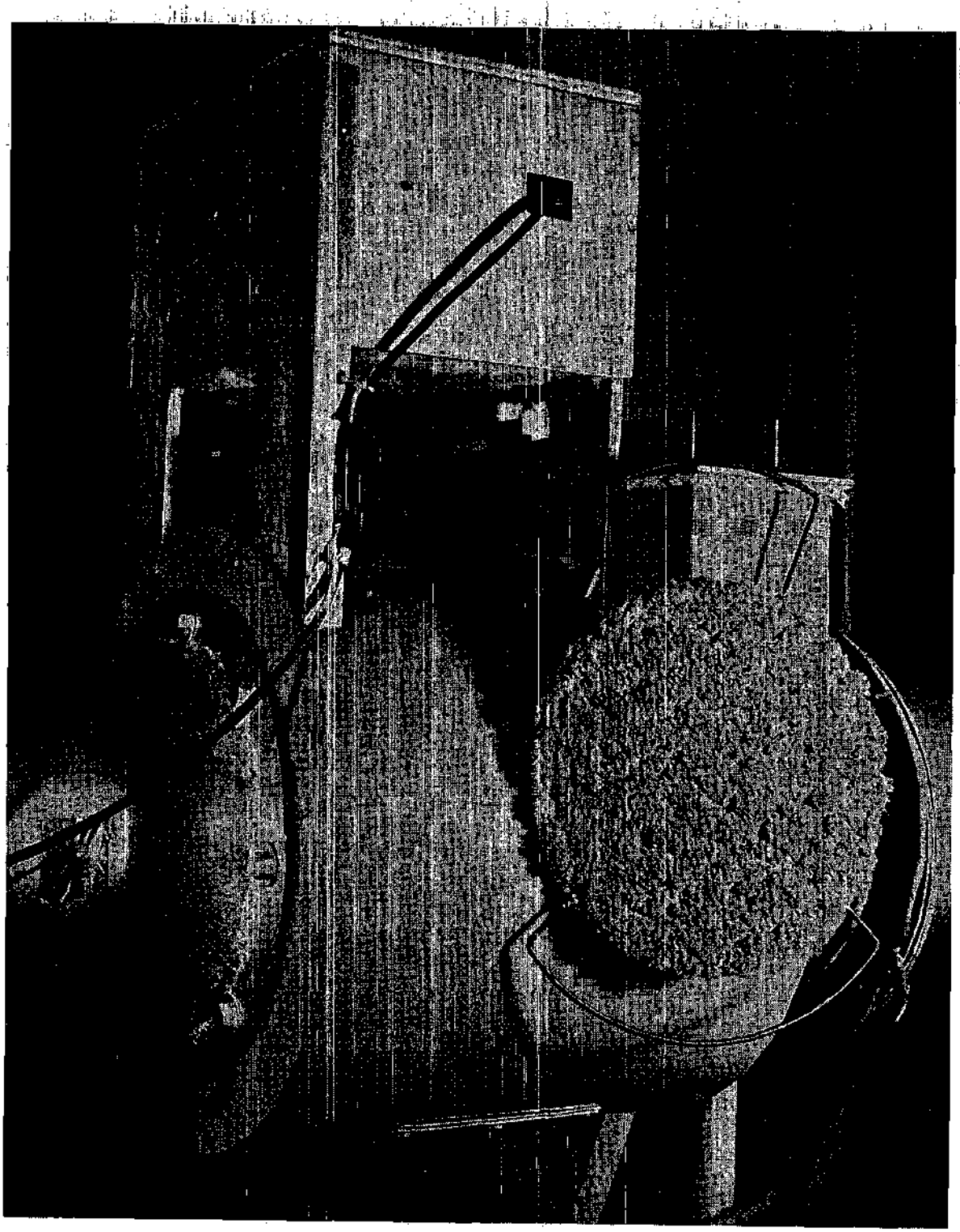

Figure 5. Sample to be Dried.

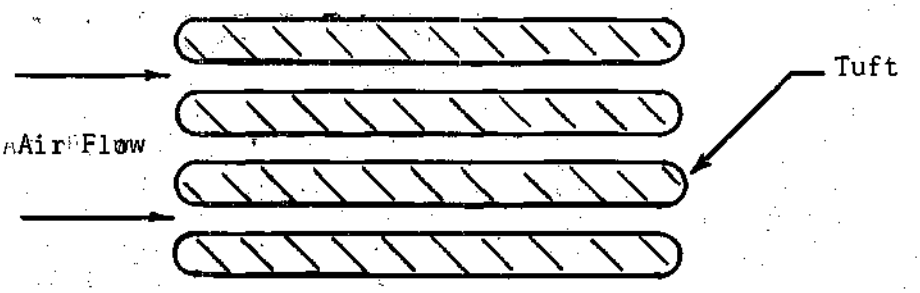

Figure 6. Model of Material to be Dried.

was observed to be a critical Reynolds number for which these effects began to show marked increase. Westervelt (13) postulated that the rate of convection heat transfer becomes appreciable only under circumstances in which the vibration is of sufficient intensity to alter the fundamental character of the flow in the neighborhood of the heat-transfer surface. This is based on the theory that the inner streaming boundary layer collapses when a critical sound-pressure level is reached. However, Fand (6) offers a second theory that the increase in heat transfer from a horizontal cylinder is due to thermoacoustic streaming.

Actual industrial drying with sound was begun by Greguss (5) who used ultrasonics to dry raw cotton. Recent studies by Boucher (2) indicate that in using a sound field of 8 k.c. and 147 to 152 db for the desorbtion of silica gel, the drying time could be reduced from 30 minutes to less than five by the use of ultrasonics instead of oven drying.

The second phenomena involved in the drying of carpet is that of mass transfer. Certainly once the surface of the sample is dry, the

remaining moisture must diffuse to the surface to be evaporated or to diffuse into the main stream.

Fussell (4) has studied the influence of sound on mass transfer rates from cylinders located traversely to the sound field and reports an apparent increase of 9 fold in the "j" factor for mass transfer.

The through-flow drying of carpet, without sound, was investigated by Brock (3), who reports that the drying rate increases directly with increases in velocity and exponentially with increases in mass-transfer coefficient. Other variables affecting the drying rate were air temperature, free stream humidity ratio, and moisture content of the carpet. Higher temperatures which led to correspondingly larger differences in humidity ratio led to higher drying rates. Increases in air humidity lowered the drying rate. This effect was most pronounced at lower air temperatures where the difference between the wet- and dry-bulb temperatures of the air were of the order of 30° F or less. The moisture content of the sample was found to affect drying rates since additional moisture absorbed in the fibers tended to cause shrinkage and decrease the net through-flow area of the sample. This resulted in higher velocities through the sample.

CHAPTER II

INSTRUMENTATION AND EQUIPMENT

A diagram of the equipment used is shown in Figure 7. The air moving apparatus was essentially the same as that used by Brock (3). Changes were made in the weighing section and in the weight sensing apparatus. Sound generation equipment was also added.

Air Moving Apparatus

Air was supplied to a 15 foot long, 12 inch inside diameter test section by a New York Blower No. 152 backward-curved blade fan. The flow was regulated by an opposed blade outlet damper. The blower was also equipped with an adjustable pulley making possible a wider range of air flow rates. A rubber connection between the fan and the test section damped out blower vibrations.

The air entered the blower through a six foot inlet duct section as shown in Figure 8. An eight inch diameter, sharp edged orifice plate was mounted at the inlet of the duct. The downstream pressure taps of the orifice plate were placed eight inches past the opening as recommended by Spink (11). The pressure drop across the orifice plate was measured by a two inch Ellison inclined draft gage. This gage was calibrated to read pressure differences of up to two inches of water to the nearest one hundredth of an inch.

The fan then discharged into three No. 3024 steel-fin exchanger sections in series in which the air could be heated up to 300^{o} F by

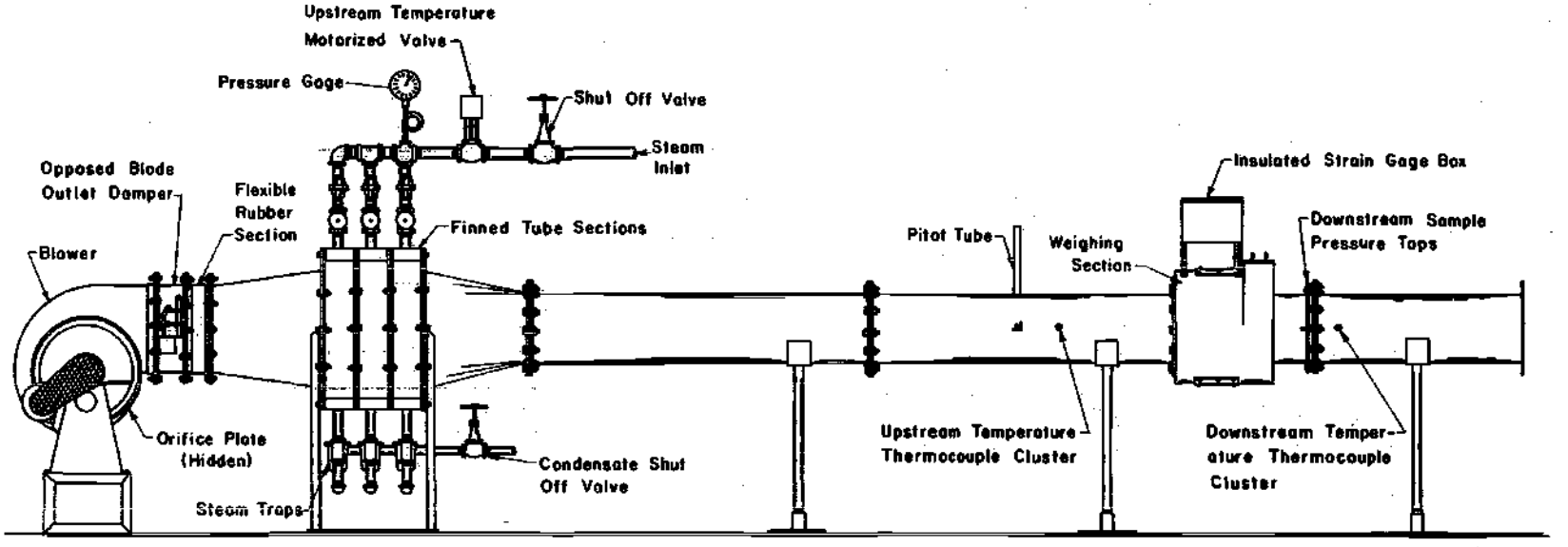

Figure 7. Schematic of Wind Tunnel Dryer.

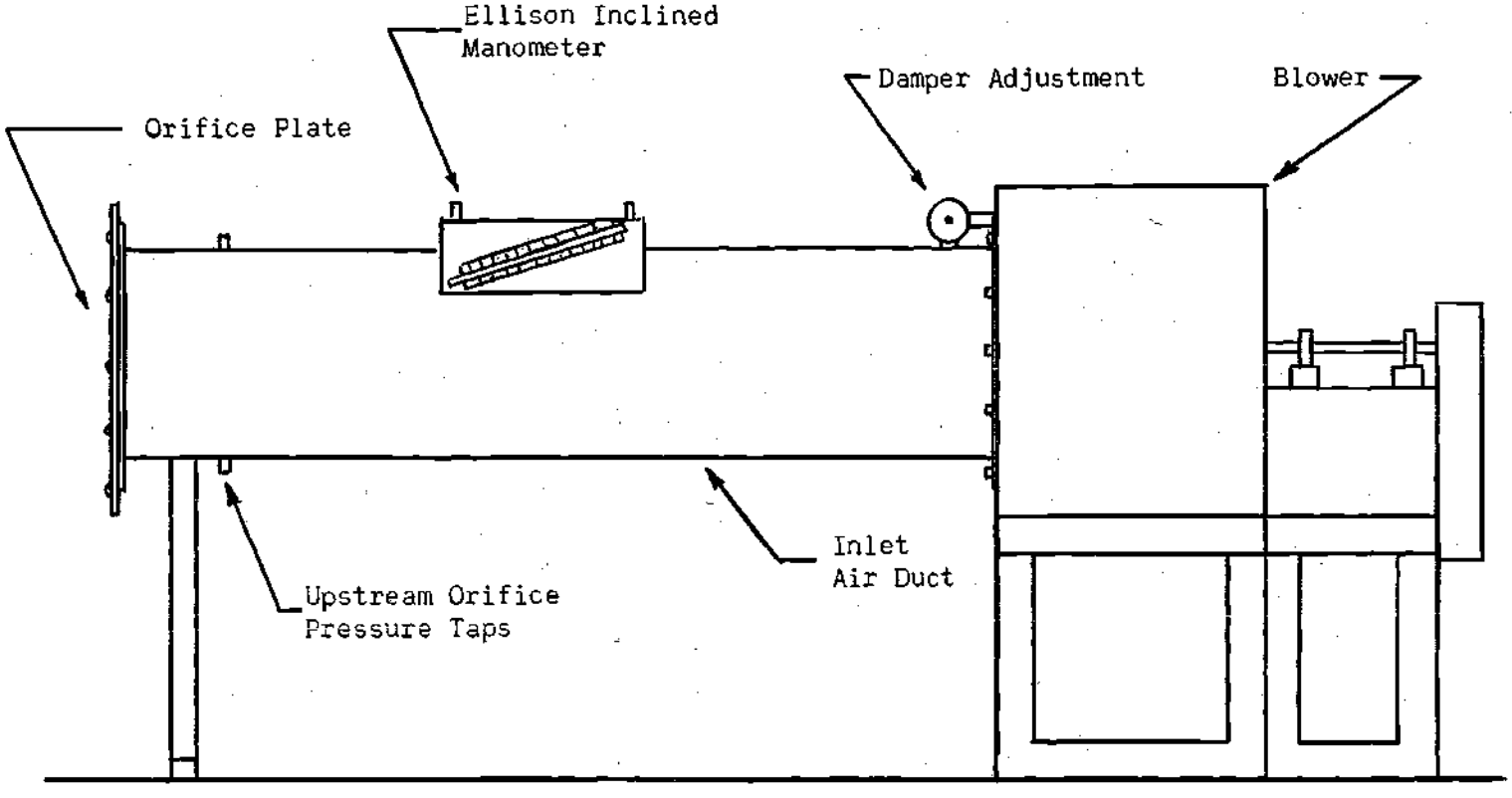

Figure 8. Schematic of Inlet Air Duct and Blower.

using condensing steam at a maximum pressure of 150 psig as the heating medium.

The temperature of the air upstream of the test section was controlled by a Minneapolis-Honeywell three-mode Electro-Line control unit and Electronik recorder operating from three No. 28 gage chromel-alumel thermocouples one foot upstream of the weighing section. The thermocouples were connected in parallel to indicate the average upstream dry-bulb temperature of the air. The Electro-Line control unit controlled the steam flow to the exchanger sections through a Minneapolis-Honeywell Model 1-1/2 - 800 motorized valve. A diagram of the control mechanism is shown in Figure 9. It was found that when the flow rate during a run was kept at a constant value, the temperature of the air stream could be kept within plus or minus three degrees of a given setting on the control device.

Weighing Section

A diagram of the weighing section is shown in Figure 10. The sample to be dried consisted of a one foot diameter piece of tufted carpet sewn on to a copper ring of the same diameter. The ring had a stand which positioned the sample in the center of the duct. The sample of carpet was suspended in a steel frame from four cold-rolled steel bars 0.079 inch by 1.00 inch by 8-1/2 inches long. These bars acted as cantilever beams being fixed at one end and the sample being supported in a freely-hung frame on the other end. These bars absorbed the initial weight of the weighing frame and support mechanism. The diameter of the sample in the frame was the same as that of the duct so that all of the sample was exposed to the air flow and imposed acoustic field. The

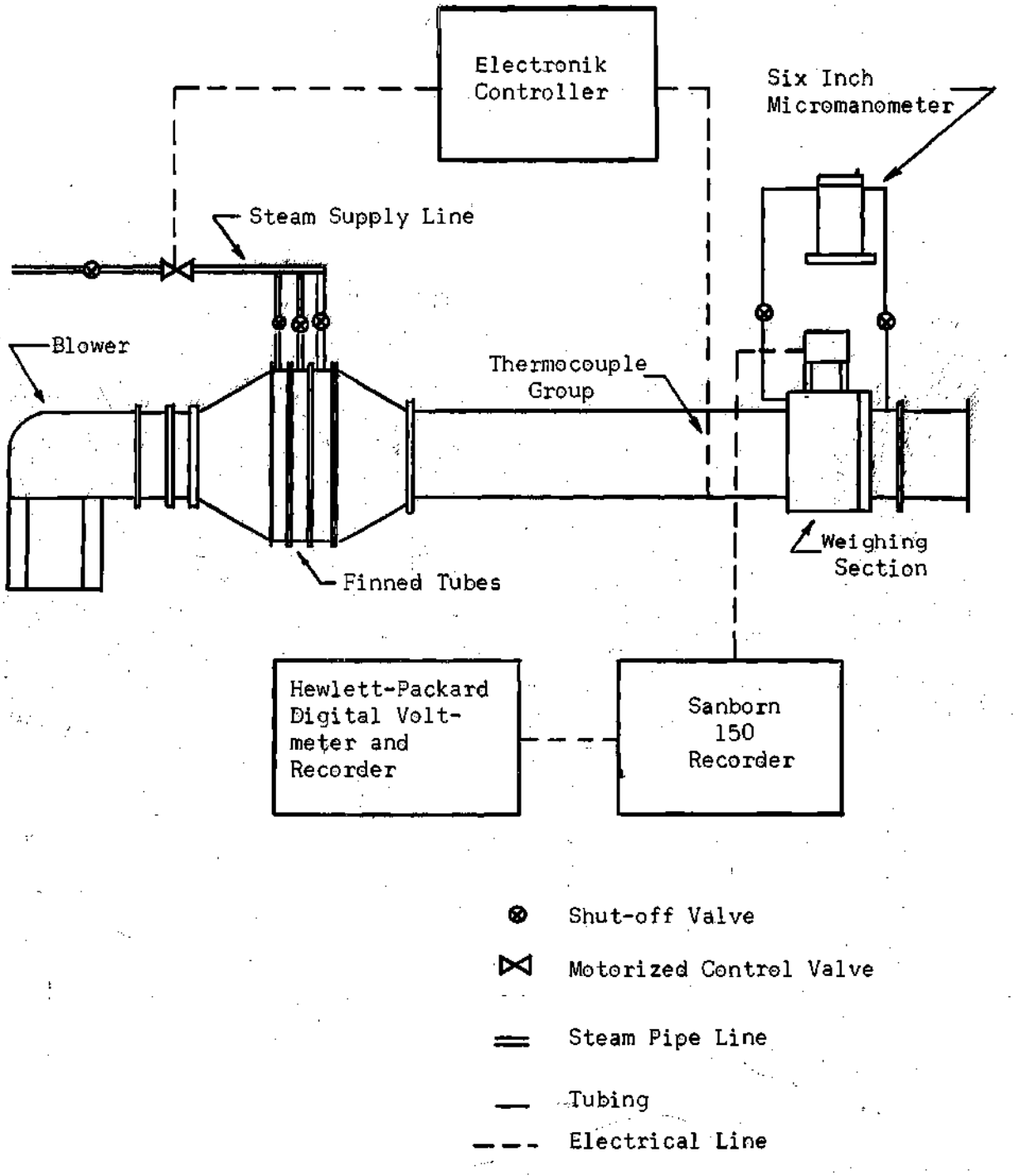

Figure 9. Schematic of Control, Measuring, and Recording Mechanism.

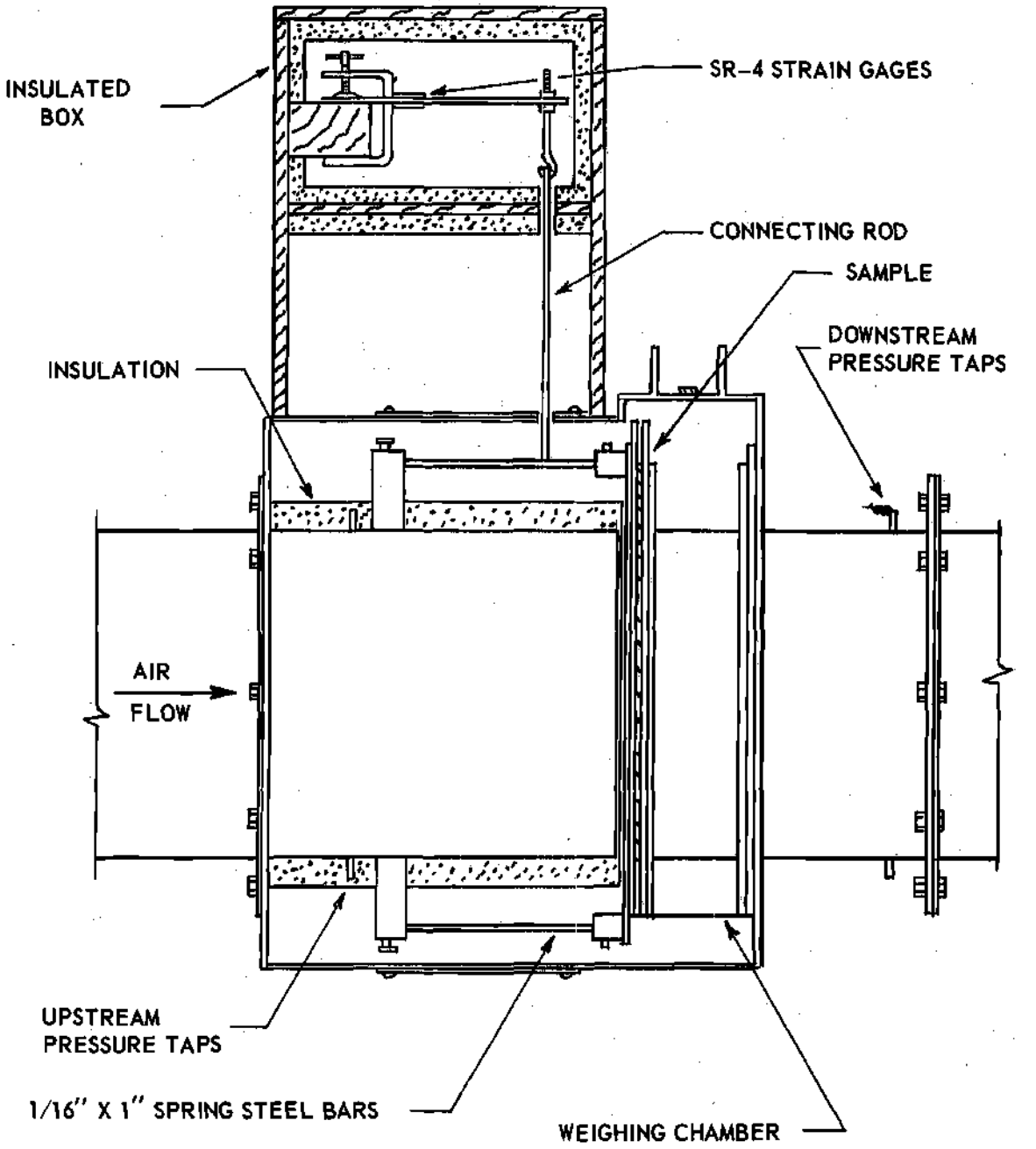

Figure 10. Schematic of Weighing Section.

support mechanism was totally enclosed to minimize air leakage and heating effects to the exterior components of the weighing mechanism.

Two manifolds with four static pressure taps spaced equally around the circumference of the duct were located upstream and downstream of the sample. They monitored the pressure drop across the sample and were connected to a Trimount six-inch micromanometer. This manometer was capable of measuring pressure differences of up to six inches of water to within plus or minus one thousandth of an inch.

A totally enclosed and insulated compartment was mounted above the weighing section as shown in Figure 10. Two cold-rolled steel bars the size of those in the weighing section were mounted as cantilever beams and connected by means of an adjustable 1/8 inch diameter rod to the weighing frame. Two Baldwin-Lima-Hamilton SR-4 type A-1 strain gages were mounted on each bar, one on top and one on bottom. The insulated compartment minimized temperature and humidity changes in the environment of the strain gages. The four gages were connected in a whole bridge for maximum sensitivity. The gages indicated a change in strain on the bars as the weighing frame was deflected. The initial tension in these bars was controlled by means of an adjustment of the length of the connecting rod in order to obtain maximum sensitivity while staying within the linear stress-strain properties of the bars.

The bridge voltage for the strain gages was supplied by a Sanborn Model 150 strain recorder and Carrier preamplifier. The output signal was then fed into a Hewlett-Packard Model 405 CR digital voltmeter with a Model 561 digital recorder. This recorder made possible the printing of the indicated voltage of the voltmeter at various sampling rates as desired by the operator.

Thus a change in weight of the sample initiated a change in strain in the support bars causing a change in resistance in the strain gages. This was reflected in a change in the output signal of the bridge which was monitored by the digital voltmeter. It was possible to monitor voltage changes of up to two volts for a one pound weight change to three decimal places with this instrument.

A second means was used at the start of this investigation to monitor the change in weight of the sample. The bridge voltage was supplied by a Brüel and Kjaer strain gage amplifier whose output signal was then fed into a Mosely Autograph Model 2-D X-Y recorder which plotted the instantaneous weight versus time. The curve obtained by using the X-Y recorder had large fluctuations which made accurate differentiation difficult.

The former method was chosen becuase of the fluctuating curve indicated by the X-Y plotter and the more favorable accuracy of the timer on the printer of the digital voltmeter as compared to the time base of the X-Y plotter, especially for runs in excess of ten minutes.

Sound Generation Apparatus

A schematic of the sound generation apparatus is shown in Figure 11. The desired frequency for resonant vibrations was generated by a RCA WA-44B audio signal generator. This device could generate frequencies from 11 cycles per second to 100,000 cycles per second. The signal was amplified by a Challenger Model CHA 75A amplifier. The wave form of the amplifier output was observed on an EICO Model 425 oscilloscope. Thus it was possible to determine the amount of distortion in the imposed wave

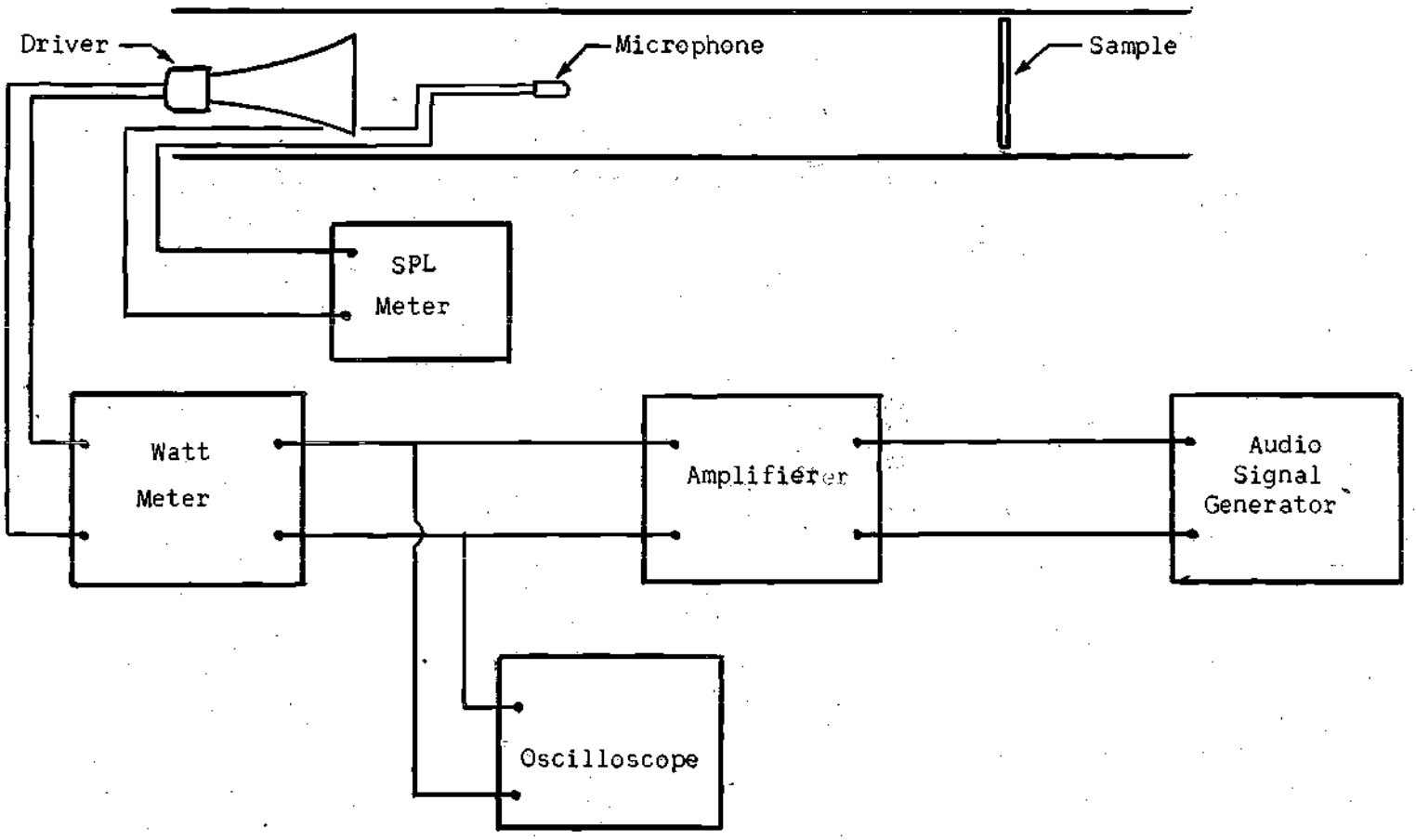

Figure 11. Schematic of Sound Generation and Measuring Apparatus.

form by the deviation of the wave observed on the oscilloscope from that of a sine wave.

The parabolic horn emitting the signal was driven by a university PA-HF 50 watt-16 ohm driver. The input power was indicated by a Heath-kit audio watt meter. A General Radio Model 9898 microphone mounted on the end of a six foot probe sensed the instantaneous sound-pressure level in the duct. This was read from a General Radio Model 1551-B sound level meter. The external calibration of the microphone and probe was accomplished by the use of a General Radio Model 1552-B calibrator.

CHAPTER III

EXPERIMENTAL PROCEDURE

Calibration of Orifice Plate

The eight inch diameter, square edged orifice plate was calibrated in accordance with the Air Moving and Conditioning Association Test Code, Bulletin 210. The orifice was located six unrestricted diameters upstream from the blower. Orifice pressure drops were measured with the inclined manometer described in chapter two. It was possible to vary the flow rate by means of a continuous adjustment on the damper of the blower and by varying the diameter of an adjustable pulley on the blower. During a specific run, the following data were obtained:

dry-bulb temperature (room and duct)
wet-bulb temperature (room)
orifice pressure drop
barometric pressure
average air velocity in duct

The average air velocity in the duct was obtained from a 20 point pitot tube traverse in both the vertical and horizontal directions. The points of measurement were obtained by dividing the flow area into ten annular rings of equal area. Calculations were then made to determine the air flow rate and a discharge coefficient for the orifice. From this mass flow rate a volumetric flow rate was then calculated based on an air density at 70° F. The volumetric flow rate was then plotted versus the orifice pressure drop. Orifice pressure drops were plotted for flow rates of 100 to 1000 cfm.

Determination of Resonant Frequencies

Drying runs were made for various sound-pressure levels in a resonant acoustic sound field. Only resonant frequencies were used during the drying runs.

To determine the conditions of resonance, it was first desired to determine the resonant frequency. With the sample out of the duct, the microphone was placed in the duct. The gain of the amplifier was turned up until a power of approximately 25 watts was indicated on the watt meter. The intensity level was then noted on the sound level meter. The frequency was varied until a sound-pressure level maximum was indicated. The microphone was moved axially to a point of maximum sound intensity. At this point, a decrease in sound-pressure level as the frequency was varied either up or down indicated a condition of resonance for the duct. The microphone was then moved axially in the duct to find the position of lowest sound-pressure level. If this position was within three inches of the sample position, the horn was moved to bring this minimum to the position of the sample. The sample was then placed in the duct and the microphone placed just downstream of the sample. The frequency was then varied to see if a sound-pressure level minimum still existed at the sample. In certain instances it did not and the frequency was changed slightly to again obtain a sound-pressure level minimum. This was taken as an indication that the sample was acting somewhat as a solid body. A sound-pressure level minimum was obtained in order to assure a velocity antinode or maximum velocity fluctuation at the sample. A diagram of the sample position in relation to the fluctuating velocity imposed by the sound field is shown in Figure 12. In certain instances

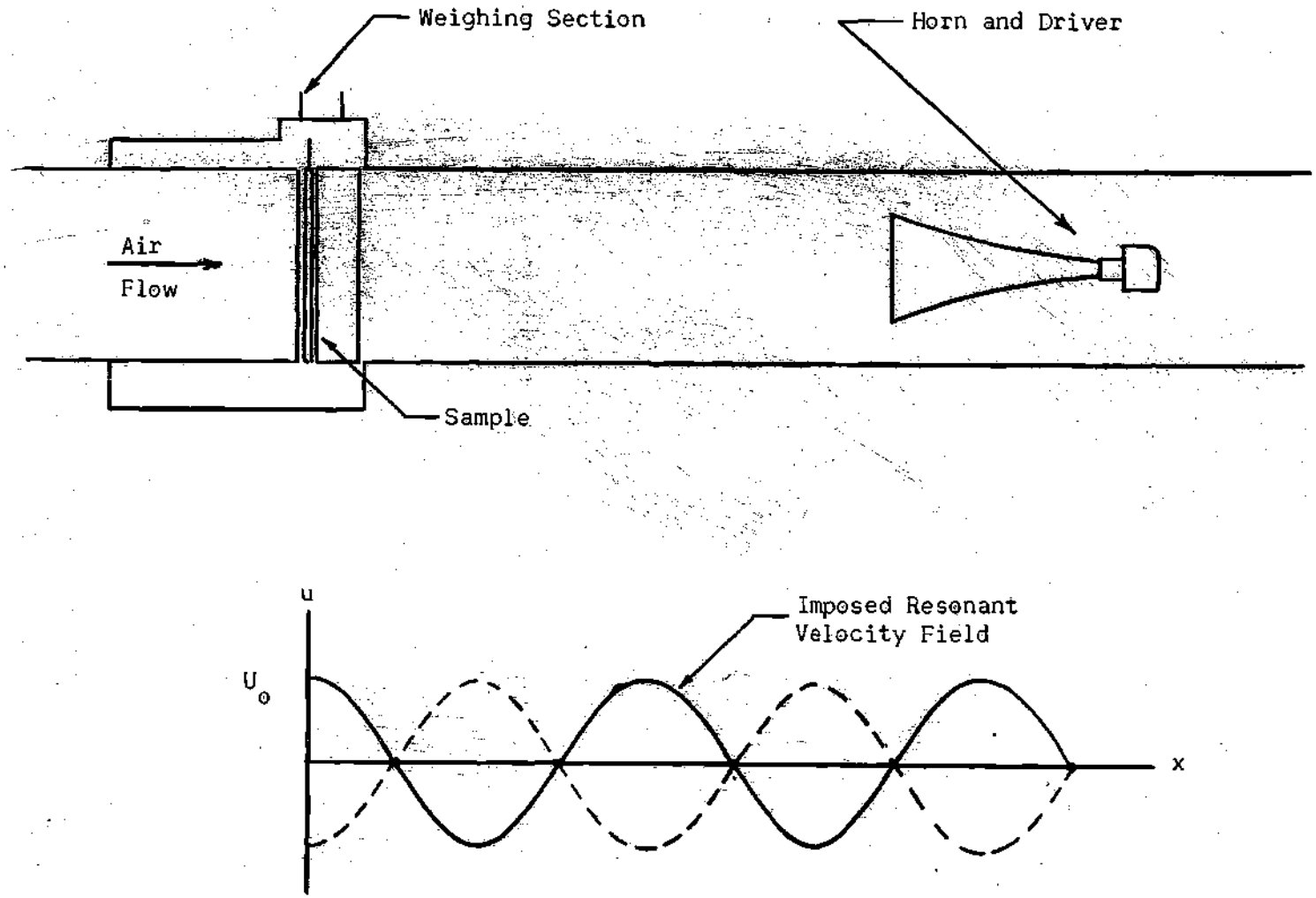

Figure 12. Schematic of Horn in Test Section.

a sound-pressure level minimum could not be placed at the sample for a particular resonant frequency due to the limited adjustment on the axial position of the horn. This point was then discarded and the procedure repeated until the desired condition existed. In each case, the resonant frequency and sound-pressure level for an input power of 50 watts was recorded.

Data was taken to determine the range of resonant frequencies for which the maximum sound-pressure level for a given power input could be obtained. For a particular enclosure, the intensity of the sound field at resonance for a specific power input will not be the same for all resonant frequencies. For frequencies ranging from 200 to 1200 cps, the maximum sound-pressure level was obtained near 300 cps. Resonant frequencies near 300 cps were therefore chosen for all drying runs.

Prerun Procedure

In preparing for a drying run, it was first necessary to calibrate the instruments. This consisted of checking the reading of the sound-pressure level meter by a standard intensity emitter, the balancing of the R-C circuit of the strain gages, and adjusting the initial tension in the measuring bars for a maximum voltage change for a given weight change. The indicated voltage change for an applied one pound weight was recorded and rechecked at the end of the run to check for drift in the strain gage circuit.

The desired flow rate was set by adjusting the damper until the inclined manometer indicated the pressure drop as read from the calibration chart. The desired air temperature was obtained by setting this temperature on the Honeywell controller which would adjust the steam

valve as needed to hold the specified temperature. The apparatus was allowed to run for at least one hour prior to a series of runs to assure stability of instrument readings and flow conditions.

The sample was prewetted in a water bath to insure a well wetted sample. The sample was then dried once to determine approximate drying time and amount of moisture removal for the flow conditions of a particular set of data.

Drying Procedure

For a particular run, the drying procedure varied only in the controlled variables, i.e. mass flow rate, type of sample, sound-pressure level, and frequency of resonant vibrations. The procedure was usually to make a series of runs at fixed values of flow rate, resonant frequency, and type of sample, while varying the sound intensity level from a maximum value at 50 watts input to a no sound value. Thus the effect of sound intensity for fixed flow conditions could be studied. It was also the practice to make at least two runs under no sound conditions to insure a reliable comparison with the data for runs with sound. This procedure was then repeated for a different flow rate, sample, or resonant frequency.

To begin a specific run, the wet sample was allowed to drip to a specific moisture content and the wet weight of the sample was then recorded. This initial moisture content was held constant for a specific series of runs. For example, the initial moisture content of sample No. 2 for data taken at a resonant frequency of 300 cps was held at 280 per cent.

With the desired flow conditions being obtained by preliminary operation with a dummy sample in the duct, the wet sample was placed in the duct and the record of its weight started on the digital voltmeter. During the run, the following data were taken:

dry-bulb temperature (room and duct)
wet-bulb temperature (room)
orifice pressure drop
sample pressure drop
drying time
sound-pressure level
frequency of resonant sound field
power input to driver

The weight of the sample and in certain instances the sound-pressure level were monitored continuously during a run.

Due to the decrease in the pressure drop across the drying sample, the position of the damper had to be continually changed during a run to maintain a constant flow rate. The sample was considered dry when no further change in the indicated weight of the sample could be observed. The weight of the dry sample was then recorded and the sample prewetted while the conditions for the next run were obtained.

CHAPTER IV

DISCUSSION OF RESULTS

Drying Rates Without Sound

The effect of a resonant sound field on drying characteristics of the material was determined by a comparison of data obtained from drying runs with an imposed resonant sound field with data from no-sound runs under the same conditions of net through-flow rate, free stream temperature, and initial moisture content of the sample.

The data obtained for each drying condition is presented in Tables 1, 2, 3, and 4 in Appendix A. Graphic representation of data is shown in Figures 13 through 24 in Appendix B.

The drying curves obtained with no imposed sound field exhibit all the regions of the drying curve shown in Figure 2. The effects of free stream temperature, flow rate, and humidity on drying rates were the same as indicated by Brock (3). It was not possible to compare exact values of drying rates as Brock used flow rates in the order of 800 cfm and this investigation studied through flow rates in the order of 300 cfm.

Drying Rates with Sound

A typical drying curve for sample number three is shown in Figure 13 where moisture content of the sample is plotted versus time dried. The drying rate curve for this run is shown in Figure 14 and was obtained by differentiating Figure 13 with a Gerber Model D-2 Derivimeter and plotting the slope versus the moisture content. The effect of sound-

pressure level on the different regions of the rate of drying curve can be observed from Figures 15 through 19.

Initial Adjustment Period

No definite trend could be determined as to the effect of the imposed sound field on the initial adjustment period. This could be attributed to the dependence of drying rates in this region upon the initial temperature of the moisture. If the initial temperature of the moisture was very near the saturation temperature corresponding to the partial pressure exerted by the water vapor, the initial adjustment period would be very short and the drying rates would be very close to that during the constant rate period regardless of any imposed sound field. A large percentage of the drying in this region takes place by the mechanical removal of liquid moisture from the sample and since there is no specific driving force as in the case of heat transfer or diffusion, a correlation between mechanical removal and an induced sound field would be difficult to obtain. Also, in commercial dryers, the use of mechanical extractors has minimized the length of drying time in this period so that it is negligible in most cases.

Constant Rate Period

The effect of a resonant sound field on drying rates in the constant rate period is shown graphically in Figures 15 through 19 and Figure 20. Figures 15 though 19 each show a set of drying rate curves for which the free stream temperature, flow rate, and initial moisture content have been held constant. Each curve represents a constant sound-pressure level which ranged from no sound to a maximum of 140 db. Tables 1 and 2 give the drying conditions for these curves.

The data show that the effect of a resonant sound field on drying rates during the constant rate period is an increase in the drying rate with sound-pressure level when other drying conditions are held constant. Tables 3 and 4 give the percentage increase of the drying rate for the constant rate period based on the drying rate for the no sound run. The maximum increase was in excess of 22 per cent.

Figure 20 shows the variation in the per cent increase of the drying rate for the constant rate period as a function of the ratio of a sound Reynolds number, Re_s, to a net through-flow Reynolds number, Re_{tf}. The sound Reynolds number is based on the maximum amplitude of the particle velocity, U_o, as calculated by equation 1.2. The mean through-flow Reynolds number is based on the average through-flow velocity determined from the net volumetric flow rate. Both Reynolds numbers are based on the duct diameter and all properties are evaluated at the dry-bulb temperature of the air upstream of the weighing section. The per cent increases plotted were taken from Figures 15 through 19 and are listed in Tables 3 and 4 in Appendix A.

The result is seen to be a straight line with a positive slope. Thus the increase in drying rate was found to vary linearly with the ratio Re_s/Re_{tf} during the constant rate period. The correlating equation for these data can be written as

$$I = 180 \frac{Re_s}{Re_{tf}} - 36.5 \qquad (4.1)$$

where I is the per cent increase in the drying rate during the constant rate period. An extension of this relation predicts increases in excess

of 50 per cent for Re_s/Re_{tf} approximately equal to 0.50. The data presented are for differences in wet- and dry-bulb temperature ranging from 19 to 45° F, for flow rates from 315 to 450 cfm, and for two carpet samples.

Certain data points are not shown because of experimental error. The voltage change during a drying run divided by the weight of moisture removed was checked against a calibration value for the digital voltmeter and if these values differed by more than 10 per cent, the data were disregarded.

It is observed from Figure 20 that increases of less than five per cent would be obtained for values of the ratio Re_s/Re_{tf} less than 0.23. This may then be taken as an approximate value for a threshold value of this ratio in order to obtain significant increases in drying rates.

A correlation between the imposed sound field and the increase in drying rates during the constant rate period can be seen in Figures 21 through 24. These are drying curves for runs 13 through 17 with sample 2. Also on each graph is a plot of the instantaneous sound-pressure level measured at a pressure antinode downstream from the sample. In each case the sound-pressure level increased rapidly until the sample had reached the critical moisture content and then the rate of increase declined and finally reached a maximum as the sample became dry. The explanation for this result is in the amount of energy absorbed by the sample.

Aso and Kinoshita (1) discuss two methods whereby acoustic energy is dissipated when a sound wave is absorbed by a fabric. One is the viscous resistance type in which absorption occurs because energy is

dissipated in order to overcome the frictional resistance between the fiber and the air in it when the sound wave passses through a fabric. Energy dissipation also occurs because the sound wave vibrates the system composed of the sample and the elastic air space around the sample. The energy absorbed by the sample due to viscous dissipation, contributes to the vaporization of moisture from within the sample. The vibration of the sample causes a mechanical removal of moisture due to the oscillation and has its greatest effect during the unbound region of drying where a large portion of the moisture content of the material is surface moisture in the form of a saturated liquid. Energy absorption due to viscous effects would also be more pronounced during this region. The increased moisture content tends to shrink the fibers thereby decreasing the free air space within the sample through which air can pass. As the sample becomes dry, the amount of acoustic energy emitted by the driver which is absorbed by the sample decreases. The sound-pressure level continuously increases to the value previously obtained with a dry sample under the same flow conditions.

These results do not imply, however, that absorption of acoustic energy accounts for the total increase in drying rate. On the contrary, calculations to determine the amount of increase in the energy absorption rate required to vaporize the additional moisture removed from the sample during the constant rate period for a sound run shows in the case of run number nine that 140 watts would be required. The power input to the driver for this run was 50 watts or under 36 per cent of the energy required to vaporize the moisture. The increase in drying rate for this run was 22.2 per cent. Likewise for run number 10, corresponding to 26

watts input to the driver 70 watts would be required to obtain the increased drying rate. In this case the power input to the driver is less than 38 per cent of the energy required by the increased absorption rate.

If the fact that the driver is probably no greater than 50 per cent efficient and that only a certain percentage of the energy radiated by the driver and absorbed by the sample would go into vaporization of moisture are taken into account, it is clear that the absorption mechanism is not the dominant factor in the increase in drying rates. This is important economically due to the inefficiency of energy conversion of acoustic generators. The increase is therefore attributed to a combination of mechanical removal and a change in the diffusion mechanism.

The data presented in Figure 19 show no significant increase in drying rates due to the imposed sound field. This was due to a large through-flow rate of 810 cfm. The ratio Re_s/Re_{tf} is approximately 0.1 when evaluated at 138 db. A high intensity sound field is therefore not sufficient to insure large increases in drying rates, but rather the magnitude of the sound particle velocity relative to the mean through-flow velocity must be above the threshold value.

Critical Moisture Content

From Figures 15, 16, 17, and 18, the critical moisture content is observed to increase in general with an increase in sound-pressure level. This however is not attributed directly to the imposed sound field, but rather as a consequence of the increased drying rates during the constant rate period.

The critical moisture content is directly related to diffusion rates such that an increased rate of internal diffusion of moisture will

maintain saturation conditions on the surface for a longer period of time and the critical moisture content is thereby lowered. Conversely, an increase in drying rates which is not accompanied by a corresponding increase in diffusion rates, will increase the critical moisture content since internal diffusion is not sufficient to maintain a saturated surface. The decrease in critical moisture content following an increased drying rate can thus be explained.

Falling Rate Period

Data for this period did not give a positive indication as to the influence of sound on drying rates in this region of the drying curve. Although drying rates for the sound runs started higher than those for no-sound conditions due to the higher constant rate period, the curves for different sound-pressure levels were observed to cross in most cases such as in Figures 15, 16, 17, and 19. This is taken as an indication that the influence of the sound field on the diffusional process in this region is not sufficient to significantly increase the drying rate when a resonant sound field is imposed.

For a particular series of runs, the total drying time was held constant. With this restriction the final moisture content was lower for drying runs with sound than for those without an imposed sound field. Therefore it would take a longer period to dry a material to the same moisture content without sound than it would with sound holding all other drying conditions constant.

At the end of the drying run, the upper part of the sample would be dry while a small lower portion would remain wet. This led to final moisture contents in the order of 40 per cent. This was caused by a

drainage of moisture from the upper to lower part of the sample as the material became dry. The wet lower portion of the material would have a greater resistance to air flow thus causing a non-uniform air flow through the sample and non-uniform drying. The length of time required to dry the material to a specified moisture content was thus increased over what it would be in a commercial dryer with the carpet suspended horizontally.

CHAPTER V

CONCLUSIONS

The effect of a resonant sound field on the drying characteristics of a tufted textile material was to increase the drying rates with increasing sound-pressure level. The largest effect was obtained for drying rates during the constant rate period where increases of up to 22 per cent were obtained. Per cent increases in drying rates for the constant rate period were found to vary linearly with the ratio Re_s/Re_{tf}. No increases in drying rates above 5 per cent were obtained for values of Re_s/Re_{tf} less than 0.23. The absorption of acoustic energy was not found to be the dominate factor in the increase in drying rates. The increases in drying were therefore attributed to a combination of mechanical removal and a change in the diffusion mechanism.

CHAPTER VI

RECOMMENDATIONS

It is recommended that the results of Figure 19 be extended to determine an exact value for the threshold Reynolds number ratio and also the upper limit for increases in drying rates. The latter investigation would require drying with lower through-flow rates and sound fields of higher intensity. Due to the fact that present industrial dryers utilize drying temperatures of the order of 225^{o} F, it is recommended that this temperature range be investigated with higher intensity sound fields to determine whether practical applications exist in present dryers.

It is also recommended that the effect of carpet density be studied to determine whether a heavier carpet sample with its increased energy absorption would raise or lower drying rates. Here again a more intense sound field would be necessary to obtain significant velocity fluctuations through the material. It would be desirable for future investigators to determine a means of measuring the drying rates while suspending the material from a horizontal position since drying is accomplished in this position in present industrial dryers and this would eliminate the non-uniform draining of moisture from the sample.

APPENDIX A

Table 1. Drying Data Sample 3

Run Number	Dry-bulb Temperature Duct °F	Wet-bulb Temperature Duct °F	Water Removed lb	Sound Pressure Level db	Flow Rate cfm	Frequency cps
1	120	75	.48	140	327	320
2	120	75	.45	138	327	320
3	120	75	.45	ns*	327	ns
4	89	70	.38	140	315	322
5	89	70	.37	139	315	322
6	89	70	.37	137	315	322
7	89	70	.36	135	315	322
8	89	70	.365	ns	315	ns

*Refers to data for no sound condition.

Table 2. Drying Data Sample 2

Run Number	Dry-bulb Temperature Duct °F	Wet-bulb Temperature Duct °F	Water Removed lb	Sound Pressure Level db	Flow Rate cfm	Frequency cps
9	87	67	.42	140	327	322
10	87	68	.43	138	327	322
11	87	67	.44	136	327	322
12	88	66	.43	ns*	327	ns
19	75	53	.50	141	450	320
20	75	53	.49	140	450	320
21	75	53	.495	136	450	320
22	75	53	.51	ns	450	ns
23	78	62	.44	138	810	299
24	77	62	.45	137	810	299
25	78	62	.46	135	810	299
26	78	62	.45	134	810	299
27	78	61	.45	ns	810	ns

*Refers to data for no sound condition.

Table 3. Drying Results Sample 3

Run Number	Sound Pressure Level db	Water Removed lb	Drying Rate*	Critical Moisture Content %	Per Cent Increased**
1	140	.48	.21	150	10.4
2	138	.45	.20	130	5.2
3	ns***	.45	.19	130	---
4	140	.38	.14	104	21.8
5	139	.37	.135	103	17.4
6	137	.37	.135	109	17.4
7	135	.36	.130	109	13
8	ns	.365	.115	100	---

*Lb moisture removed/lb room dry sample, minute-for the constant rate period.

**For increase in constant rate period relative to no-sound run.

***Refers to data for no-sound condition.

Table 4. Drying Results Sample 2

Run Number	Sound Pressure Level db	Water Removed lb	Drying Rate*	Critical Moisture Content %	Per Cent Increased**
9	140	.42	.22	120	22.2
10	138	.43	.20	90	11.1
11	136	.44	.18	90	0
12	ns***	.43	.18	77	---
19	141	.50	.33	130	22.3
20	140	.49	.33	136	22.3
21	136	.495	.27	100	0
22	ns	.52	.27	97	--
23	138	.45	.40	70	0
24	137	.47	.41	80	2.5
25	135	.46	.40	75	0
26	134	.45	.39	80	-2.5
27	ns	.45	.40	70	--

*Lb moisture removed/lb room dry sample, minute-for the constant rate period.

**For increase in constant rate period relative to no-sound run.

***Refers to data for no-sound condition.

APPENDIX B

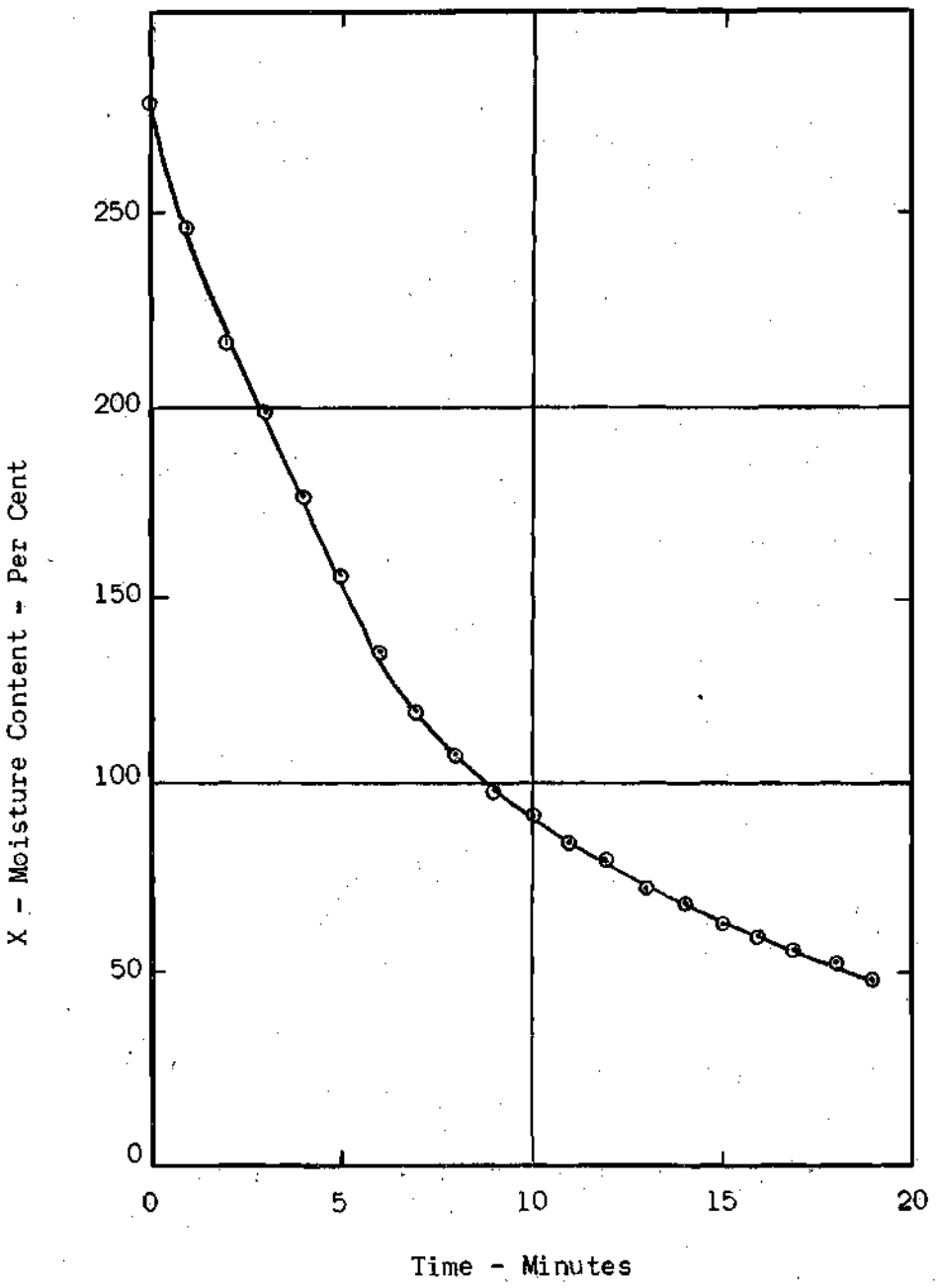

Figure 13, Drying Curve, Run 3.

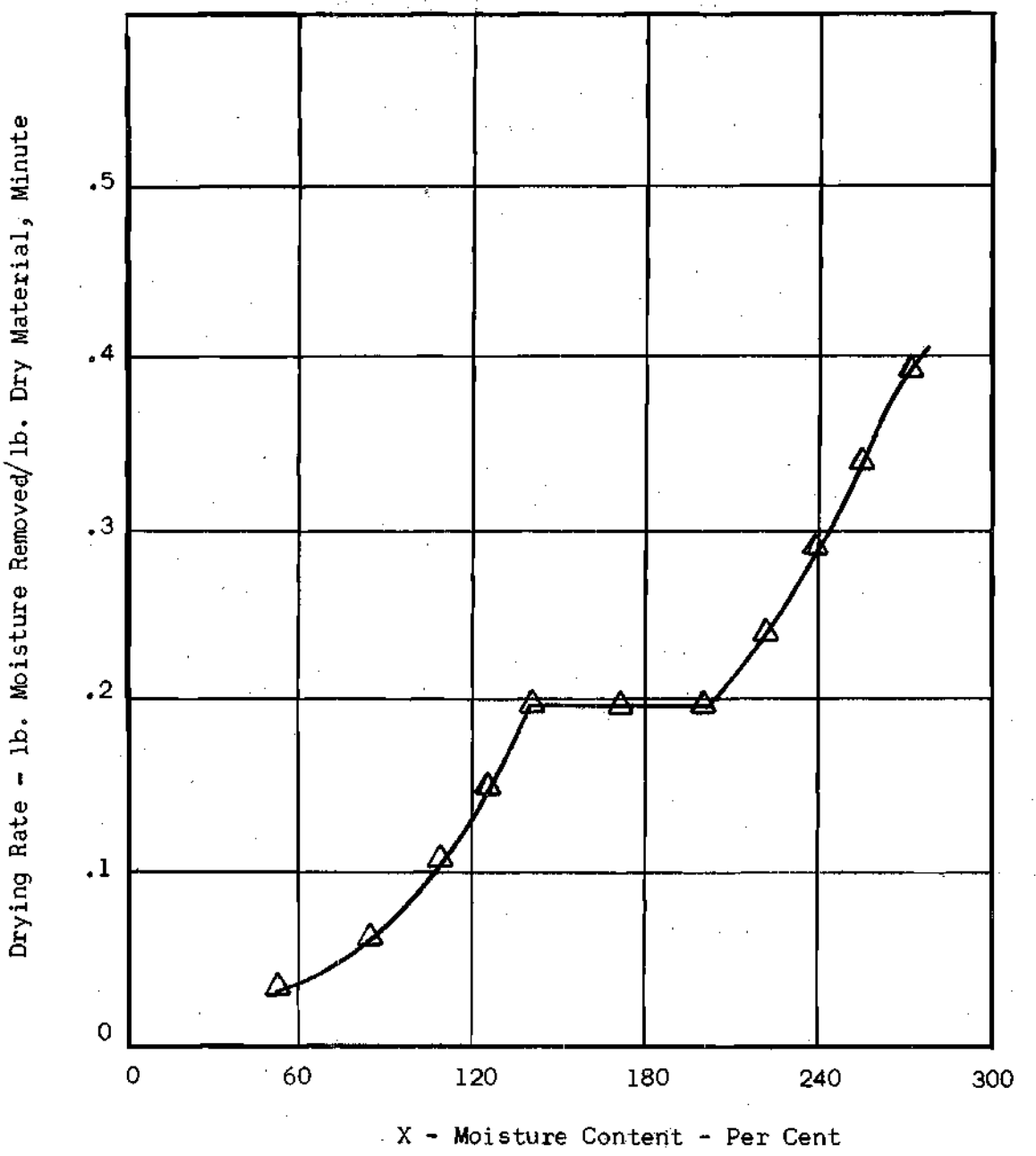

Figure 14. Drying Rate Curve, Run 3.

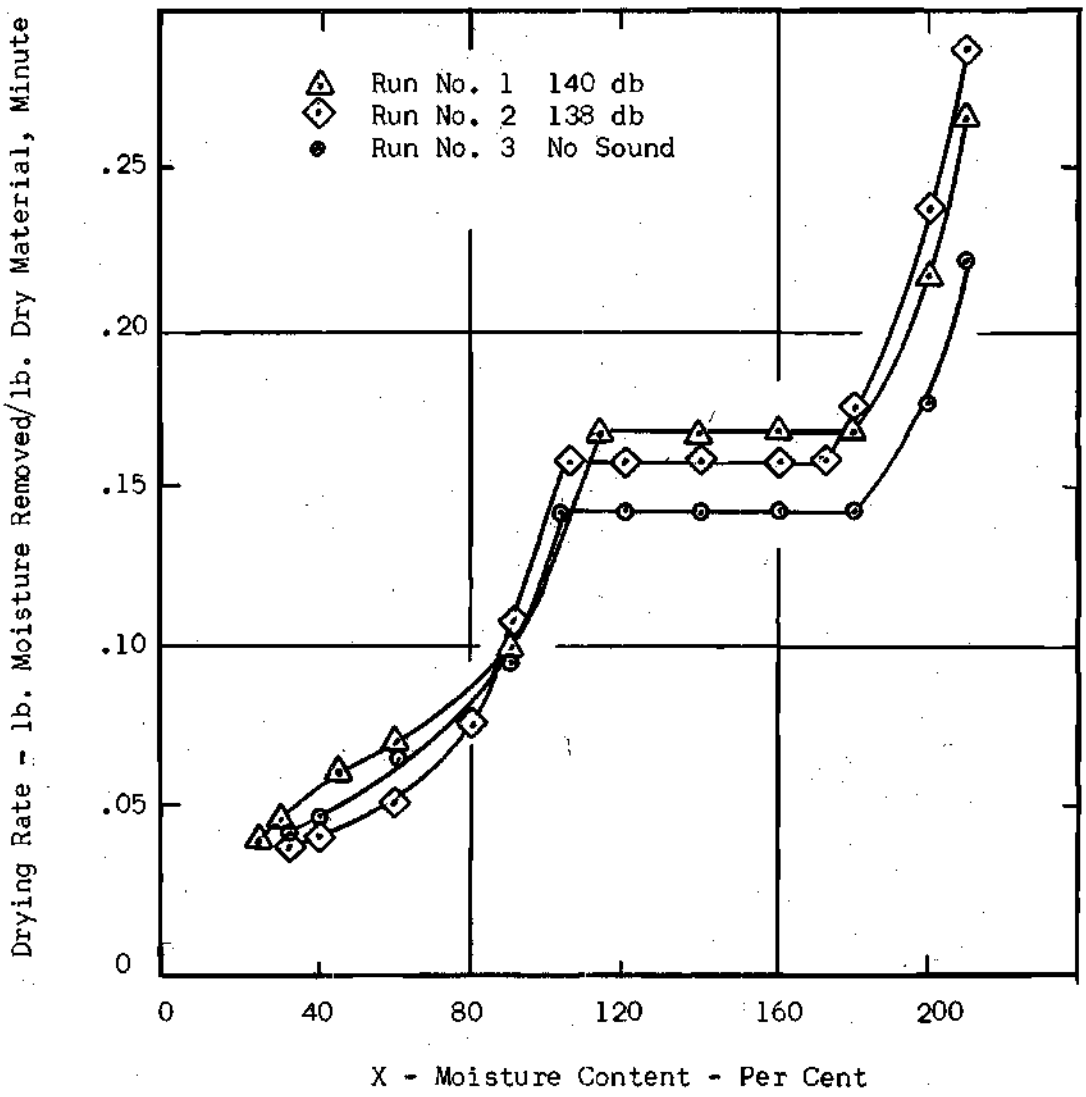

Figure 15. Rate of Drying Curves
327 cfm, Sample 3.

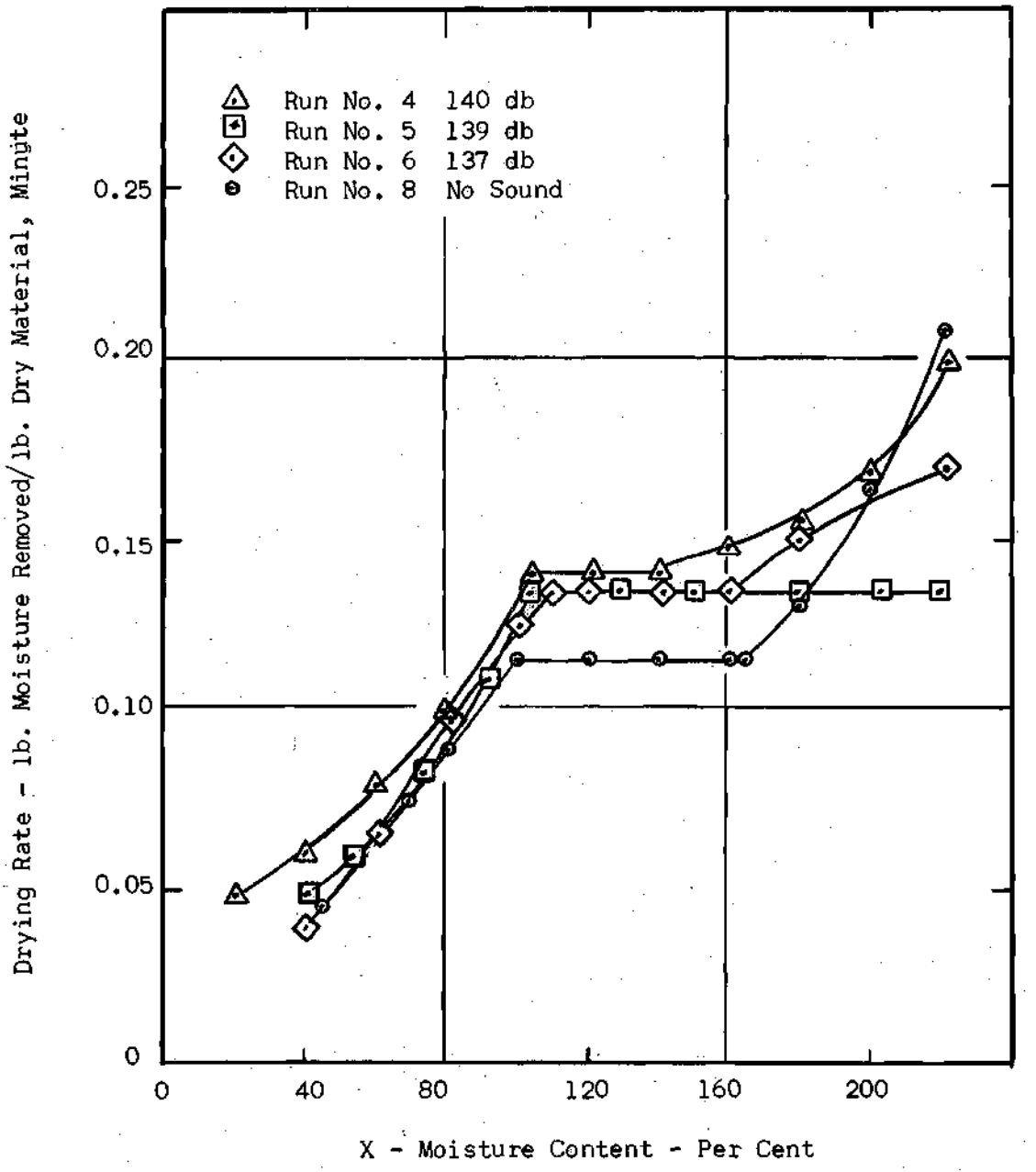

Figure 16. Rate of Drying Curves
315 cfm, Sample 3.

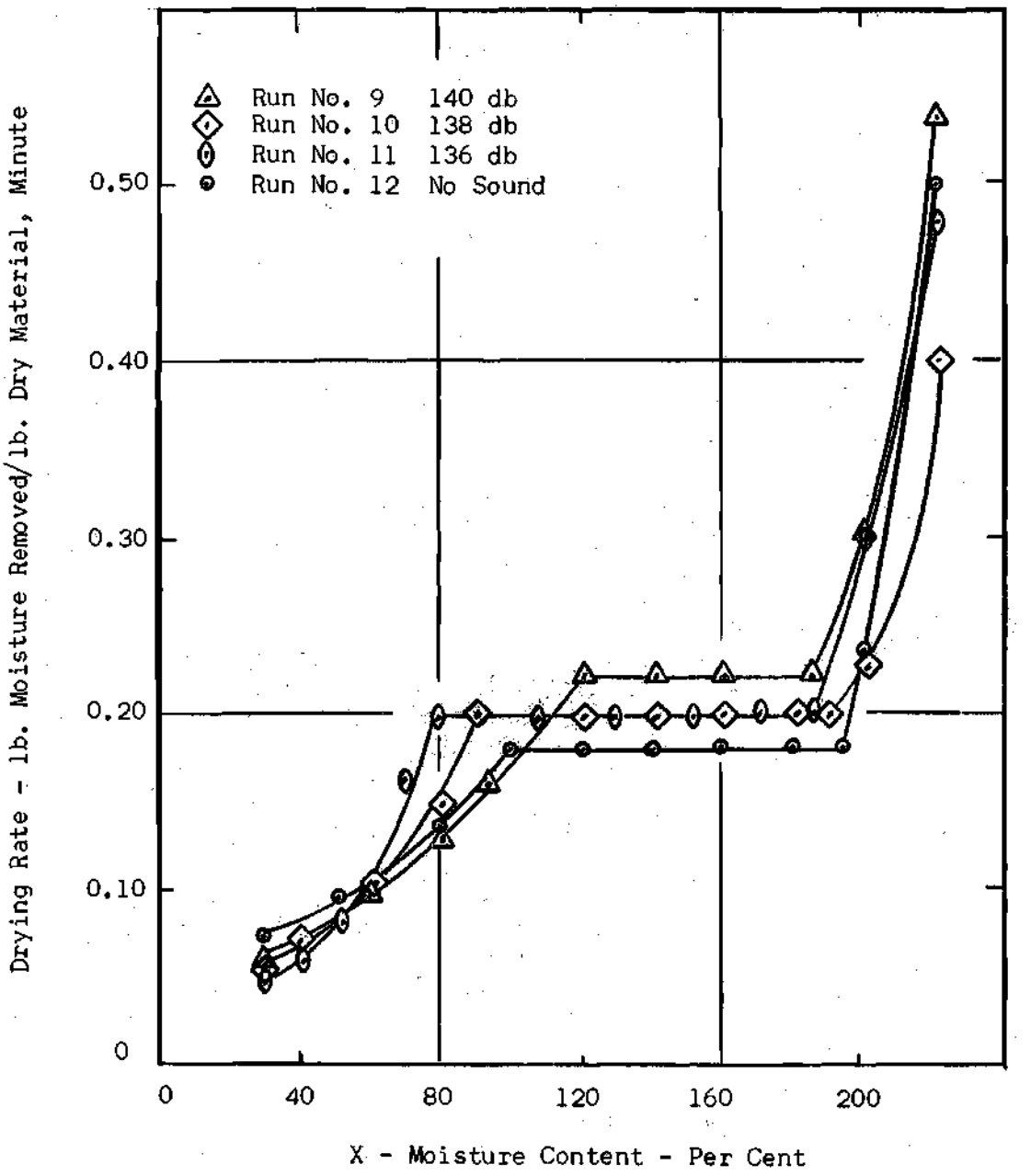

Figure 17. Rate of Drying Curves
327 cfm, Sample 2.

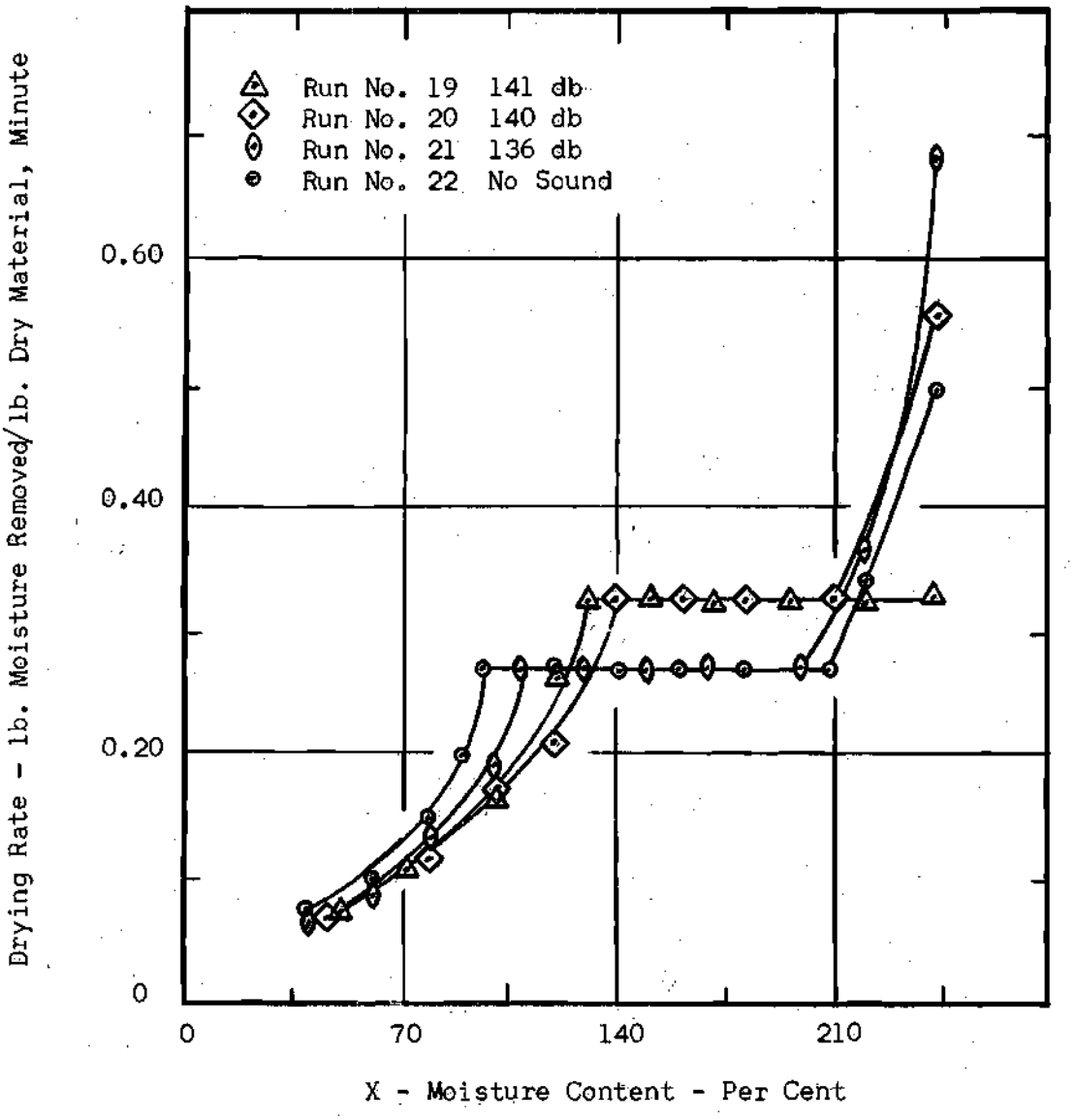

Figure 18. Rate of Drying Curves
450 cfm, Sample 2.

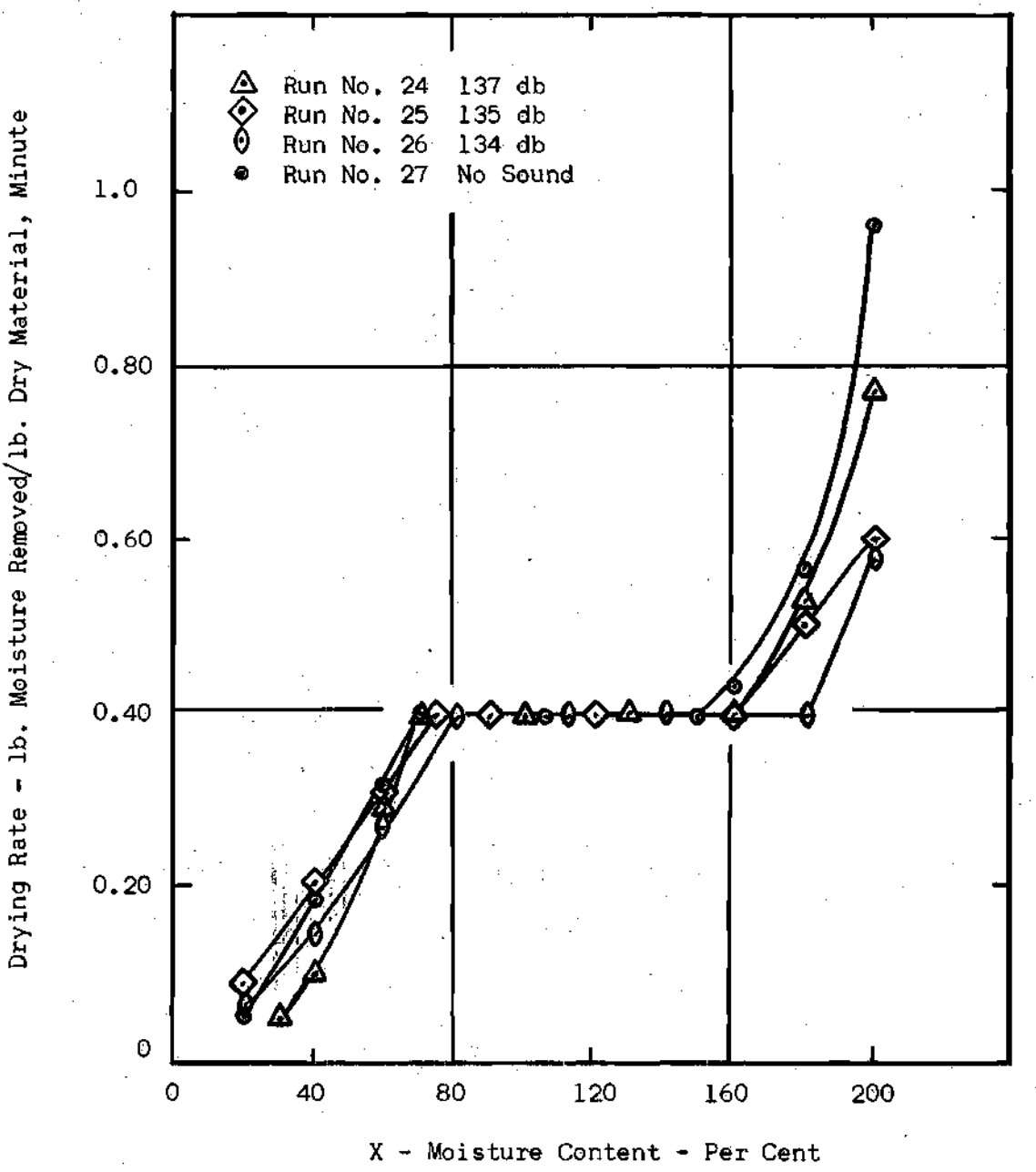

Figure 19. Rate of Drying Curves
810 cfm, Sample 2.

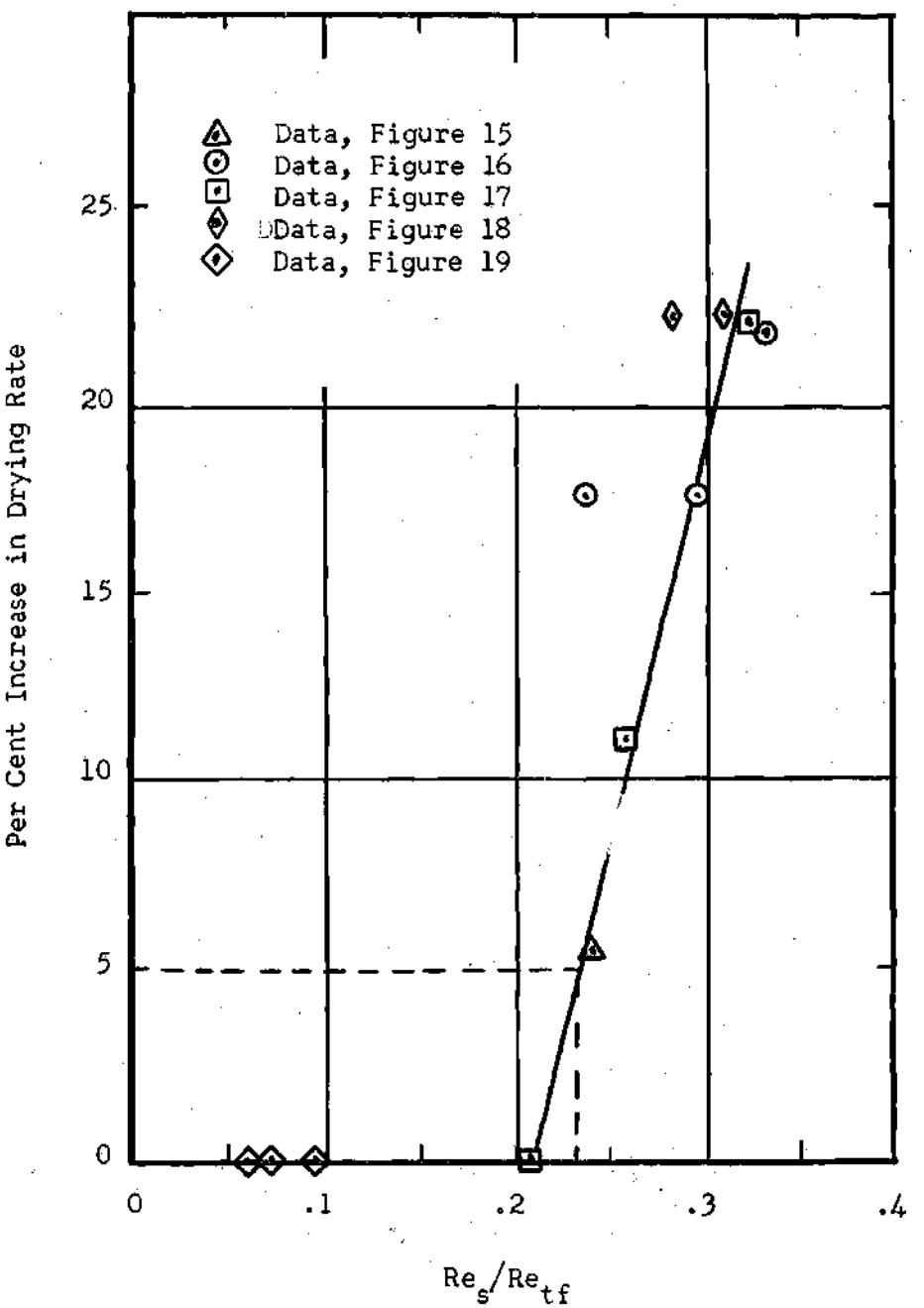

Figure 20. Per Cent Increase in Drying Rate.

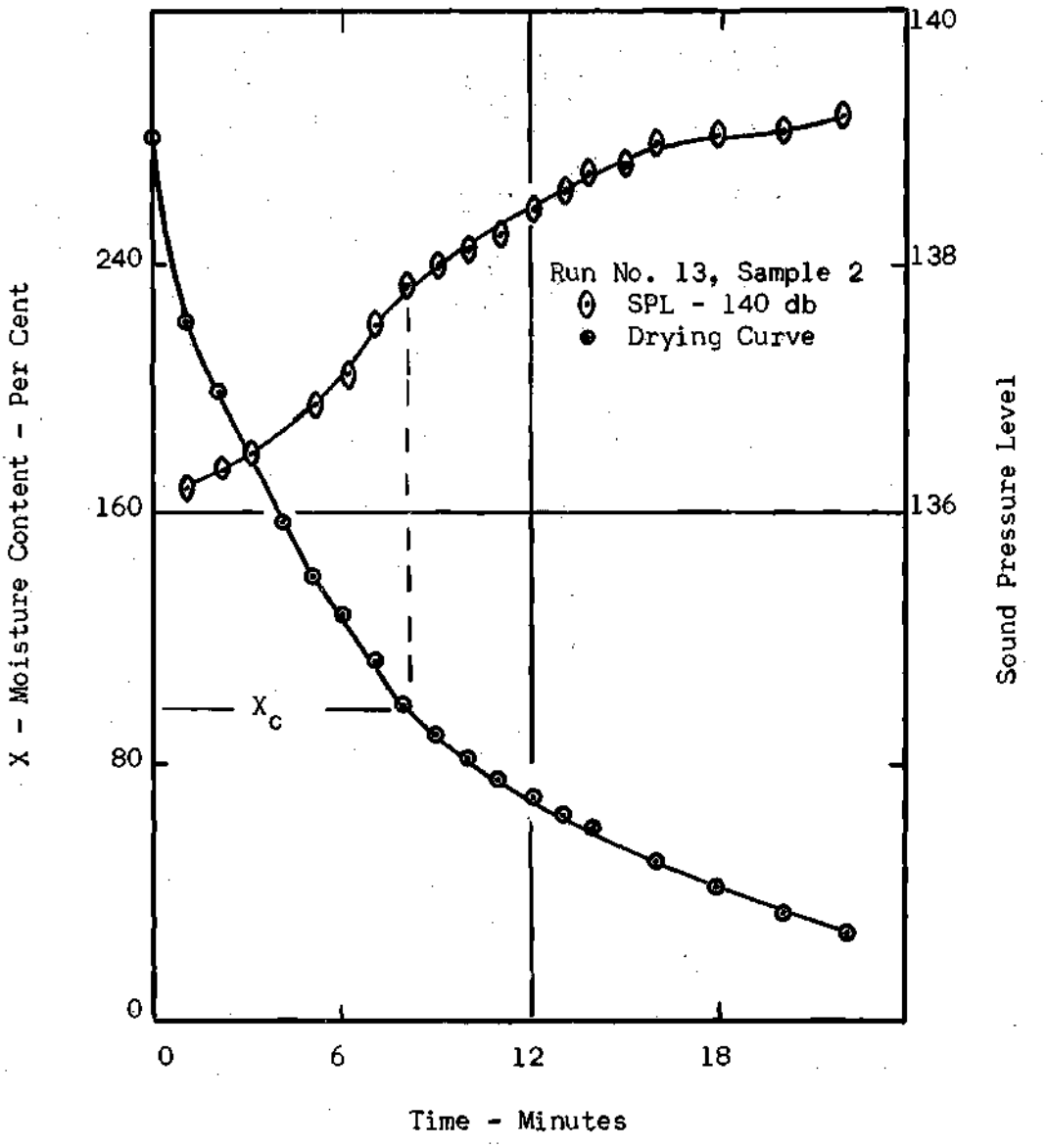

Figure 21. SPL Variation.

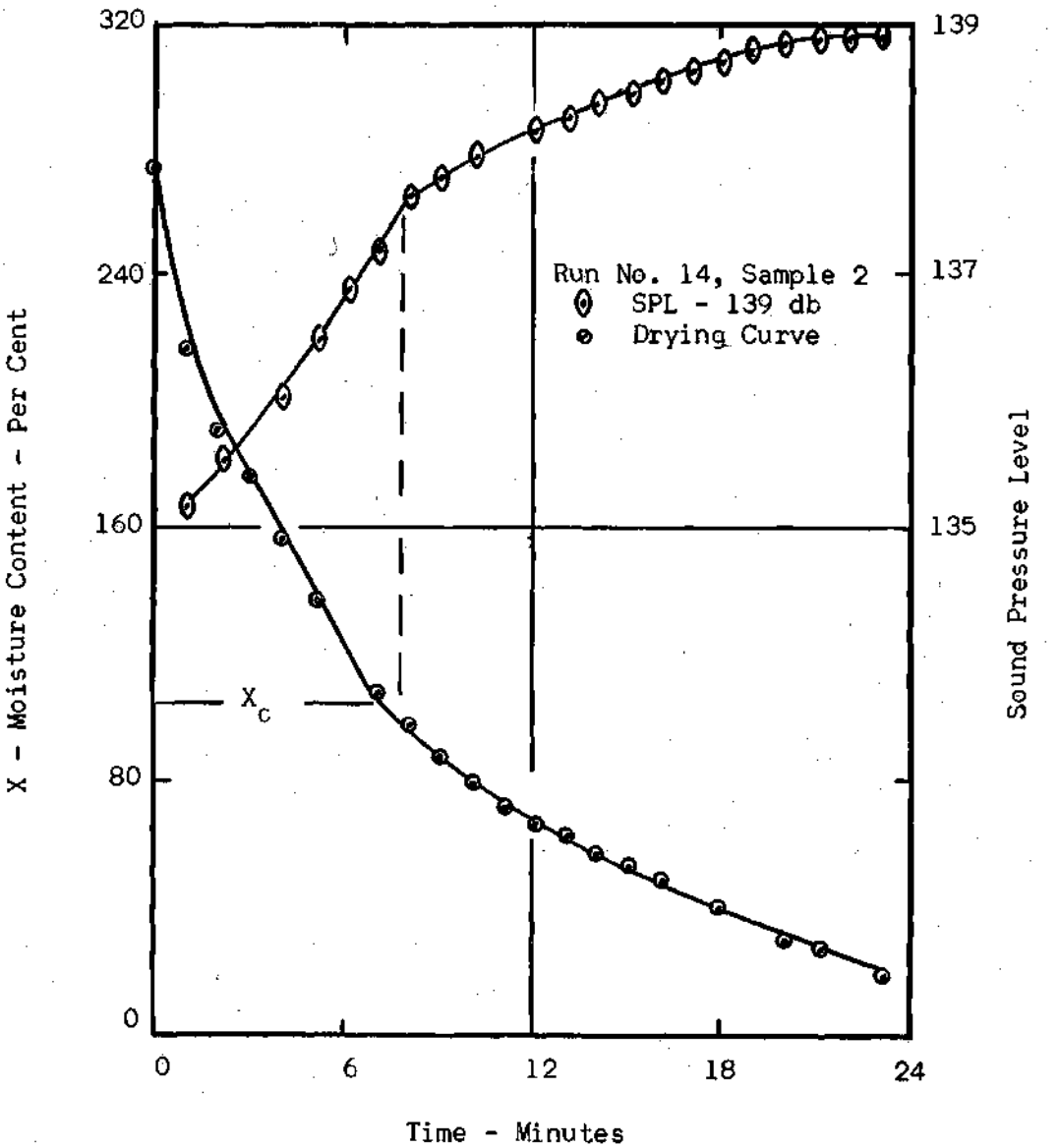

Figure 22. SPL Variation.

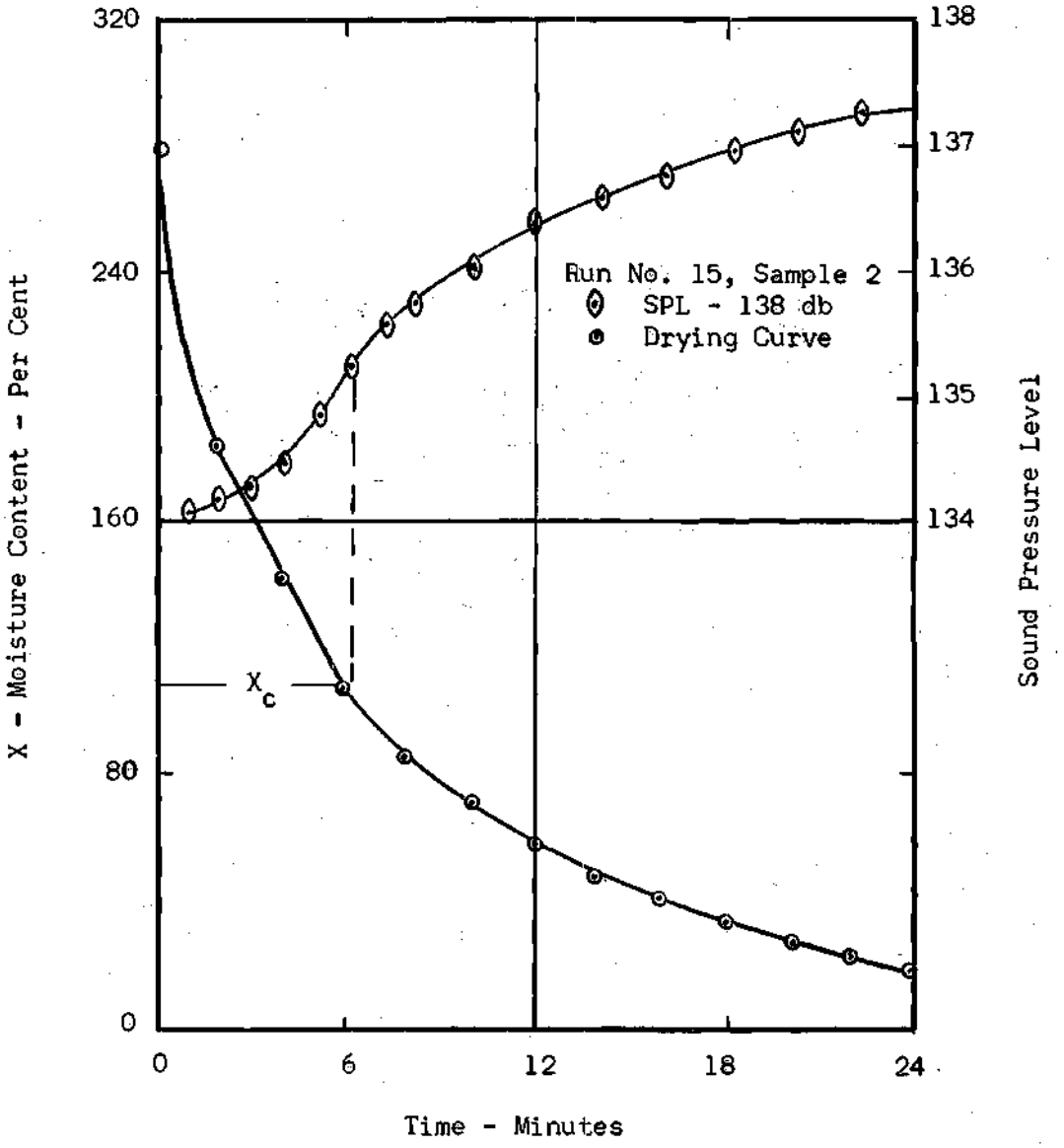

Figure 23. SPL Variation.

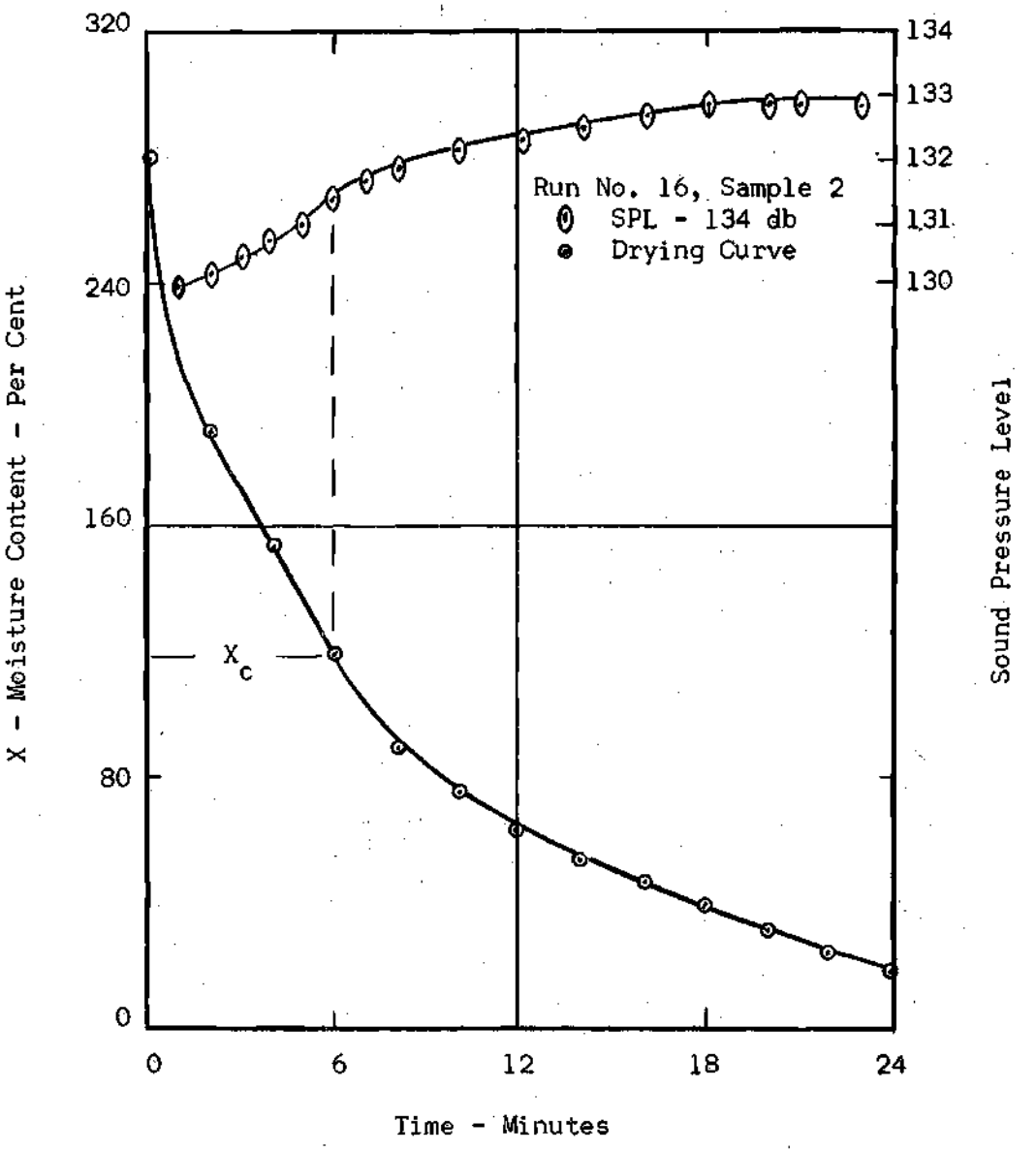

Figure 24. SPL Variation.

LITERATURE CITED

1. Aso, Sado and Kinoshita, Rikuhiro, "Absorption of Sound Wave by Fabrics," Journal of the Textile Machinery Society of Japan, Vol. 19, No. 1, 1963, p. 32.

2. Boucher, R. M. G., "Ultrasonics Boosts Heatless Drying," Chemical Engineering, Vol. 66, No. 19, 1959, p. 151.

3. Brock, Donald J., Through-Flow Drying of Tufted Textile Materials, M. S. Thesis, Georgia Institute of Technology, 1963.

4. Fussell, Delbert E., Tao, Luh C., "Sonic Effect on Convection Heat and Mass Transfer Rates Between Air and a Transverse Cylinder," Chemical Engineering Progress, American Institute of Chemical Engineers, Vol. 59, No. 41, 1963, p. 180.

5. Greguss, P., Ultrasonic News, Vol. 4, No. 4, 1959, p. 10.

6. Fand, R. M., "Mechanism of Interaction Between Vibrations and Heat Transfer," Journal of Acoustical Society of America, Vol. 34, No. 12, 1962, p. 1887.

7. Fand, R. M., Kaye, J., "Acoustic Streaming Near a Heated Cylinder," Journal of Acoustical Society of America, Vol. 32, No. 5, 1960, p. 579.

8. Hunter, T. F., Bolt, R. H., Sonics, John Wiley and Sons, Inc., New York, 1955, p. 202.

9. Martinelli, R. C. and Boelter, L. M. K., "The Effect of Vibration of Heat Transfer by Free Convection from a Horizontal Cylinder," Proceedings of the 5th International Congress of Applied Mechanics, 1938.

10. Purdy, K. R., Private communication between Dr. Kenneth R. Purdy and J. R. Dunn, Georgia Institute of Technology, Atlanta, Georgia, 1964.

11. Spink, L. K., Principles and Practice of Flow Meter Engineering, The Foxboro Co., Foxboro, Mass., 1958, p. 179.

12. Treybal, R. E., Mass-Transfer Operations, McGraw-Hill, New York, 1955, p. 524.

13. Westervelt, Peter J., "Effect of Sound Waves on Heat Transfer," Journal of the Acoustical Society of America, Vol. 32, No. 3, 1960, p. 337.